Formation of a cohesive floodplain in a dynamic experimental meandering river

W.M. van Dijk, W.I. van de Lageweg, and M.G. Kleinhans

Faculty of Geosciences, Department of Physical Geography, Utrecht University, Utrecht, The Netherlands.
woutvandijk@gmail.com

Abstract

Field studies suggest that a cohesive floodplain is a necessary condition for meandering in contrast to braided rivers. However, it is only partly understood how the balance between floodplain construction by overbank deposition and removal by bank erosion and chutes leads to meandering. This is needed because only then a dynamic equilibrium exists and channels maintain meandering with low width-depth ratios. Our objective is to understand how different styles of floodplain formation such as overbank deposition and lateral accretion cause narrower channels and prevent chute cutoffs that lead to meandering. In this study we present two experiments with a self-forming channel in identical conditions, but to one we added cohesive silt at the upstream boundary. The effect of cohesive silt on bank stability was tested in auxiliary bank erosion experiments and showed that an increase in silt reduced erosion rates by a factor of 2. The experiment without silt developed to a braided river by continuous and extensive shifting of multiple channels. In contrast, in the meandering river silt deposits increased bank stability of the cohesive floodplain and resulted in a reduction of chute cutoffs and increased sinuosity by continuous lateral migration of a single channel. Overbank flow led to deposition of the silt and two styles of cohesive floodplain were observed; first, overbank vertical-accretion of silt, e.g. levee, overbank sedimentation or splays; and second, lateral point bar accretion with silt on the scrolls and in the swales. The first style led to a reduction in bank erosion, while the second style reduced excavation of chutes. We conclude that sedimentation of fine cohesive material on the floodplain by discharge exceeding bankfull is a necessary condition for meandering.

1. Introduction

Rivers can have various channel patterns, such as braided and meandering (e.g. Leopold and Wolman, 1957; Schumm and Khan, 1972). It has long been hypothesized that cohesive floodplain material or vegetation adds strength to river banks, and that this is a necessary condition for meandering (e.g. Ferguson, 1987). Rivers with a cohesive floodplain develop into a meandering river, while non-cohesive floodplains lead to channel widening which eventually results in braiding (Parker, 1979; Ferguson, 1987; Kleinhans, 2010). Still, to experimentally reproduce a sustained dynamic meandering channel pattern in the laboratory has proven difficult, so that the exact conditions for meandering remained unclear. In the experimental work of Braudrick et al. (2009), meandering was sustained by the addition of vegetation to the floodplain. Geomorphologic evidence of meandering rivers has been found on Mars where vegetation cannot have played a role (Howard, 2009). Here we report on experiments which resulted in a braided and a meandering river, where the only difference was the addition of cohesive fines in the sediment feed.

Meandering rivers are characterized by a high sinuosity as meander bends can migrate laterally and increase the bend amplitude, while remaining single-threaded. Braided rivers have a low sinuosity and are characterized by multiple-threads. In meandering rivers, channel migration of the bends are slow (Hickin and Nanson, 1984) and bends develop in phases of creation, growth and abandonment (Camporeale et al., 2005). An important aspect of bend migration is bank erosion (Kleinhans, 2010). First, banks are undercut by fluvial erosion at the base and lower portion of the banks; second, bank retreat occurs by mass failure of the bank (Darby et al., 2000, 2007; Simon et al., 2000; Simon and Collinson, 2002). Then, the bank sediment settles at the bank toe and armoring protects the bank against fast erosion (Thorne, 1982; Parker et al., 2011) and shifts the locus of the high flow velocity, which reduces the shear stress acting on the bank (Kean and Smith, 2006a,b; Darby et al., 2010). Several studies attempted to predict bank erosion rates by calculating the bank erosion processes (e.g. Ikeda et al., 1981; Rinaldi and Darby, 2008; Langendoen and Simon, 2008; Parker et al., 2011). The strength of the bank depends on the floodplain style and floodplain cohesion. Other studies empirically linked bank erosion rates in bends to flow processes of channel depth, bend curvature, friction with the bank (Hickin and Nanson, 1984; Furbish, 1988) and the adaptation length of momentum redistribution of the flow across the curved channel (Struiksma et al., 1985). Bend migration rate generally increases when bends become sharper. On the other hand in braided rivers migration rates are high even without sharp bends (Hooke, 2003). High bank erosion rates in experiments with cohesionless sediment led to channel widening and the development of a braided river (Ashmore, 1991). There-

fore, we hypothesize that cohesive floodplains are required to have stronger banks to sustain low width-depth ratios.

Chute cutoffs, which shorten the flow path, are a limiting process in the development of highly sinuous bends. The development of chute cutoffs is described in several field studies (e.g. Constantine et al., 2010; Micheli and Larsen, 2011; Zinger et al., 2011). Furthermore, chutes have limited the development of high sinuous meandering rivers in earlier experiments (Friedkin, 1945; Peakall et al., 2007; Braudrick et al., 2009; Tal and Paola, 2010; Van Dijk et al., 2012). To sustain meandering, chute cutoffs have to be limited. Cutoffs can be prevented by vegetation growth to stabilize banks, but meandering rivers form also in areas were vegetation does not play a role, e.g. intertidal muds (Kleinhans et al., 2009), Martian rivers (Howard, 2009), glaciers (e.g. Gorner Glacier, 45°58′11″N 7°48′6″E, observation by WMvD) and deserts (Matsubara et al., 2011). Therefore, we hypothesize that cohesive sediment deposition on the point bars is a sufficient condition to prevent chute cutoffs.

Sediment erosion by bend migration and cutoff is balanced by deposition of sediment forming new floodplains. Lateral migration of the channel leads to erosion of the higher outer bank, while lateral accretion and floodplain construction on the inner side of the bend is lower (also known as floodplain shaving, Lauer and Parker, 2008). The process of floodplain shaving and channel extension results in local differences between erosion and deposition. This difference is balanced by overbank deposition or by filling depressions (e.g. abandoned channels, Lauer and Parker, 2008). Floodplains of silt and clay are constructed during floods (e.g. Middelkoop and Asselman, 1998) with more deposition near the channel and a general decrease of fine deposition with increasing distance from the channel (e.g. Walling and He, 1997; Törnqvist and Bridge, 2002). This shows that to build a cohesive floodplain, flow discharges are required that at least temporarily exceed bankfull height, so that fines deposit on the high non-cohesive banks and in the disconnected lows to balance the local differences in elevation.

Construction of a new floodplain can occur in different styles. First, an important process in this context is lateral point bar accretion (Nanson and Croke, 1992) on the inner side of the bend, which forms scroll bars that, with overbank deposition, becomes a floodplain (Jackson, 1976; Nanson, 1980). This floodplain consists of varying grain-sizes and is mostly occupied during high flow stages (Nanson and Croke, 1992). Second, overbank flow on the outer bank and at the edge of the channel forms vertical-accretion (Nanson and Croke, 1992), e.g. levees and splays (Brierley et al., 1997; Cazanacli and Smith, 1998). These splay could build out forming crevasses, but could also lead to avulsion (Pérez-Arlucea and Smith, 1999). Overbank sedimentation produces a floodplain that consist of a non-cohesive bed with a cohesive layer on top. Abandoned channels are filled by deposition of relatively coarse sediments that build plug bars (Toonen et al., 2012). After disconnection, finer sediments fill the remaining depressions (e.g. Lewis and Lewin, 1983). An experimental test of the construction of a cohesive floodplain and how bank stabilization leads to a meandering river has not been done to date.

Earlier studies have shown that the addition of bank cohesion decreases channel migration and changes channel width-depth ratio when bank stability increases (Friedkin, 1945; Schumm and Khan, 1972; Smith, 1998; Gran and Paola, 2001; Peakall et al., 2007; Braudrick et al., 2009; Tal and Paola, 2010). However, in prior experiments bank strength was provided by adding cohesive sediments or vegetation seeds manually on top of the floodplain (Friedkin, 1945; Schumm and Khan, 1972; Gran and Paola, 2001; Braudrick et al., 2009; Tal and Paola, 2010). In an earlier experiment (Van Dijk et al., 2012) we showed the development of a meandering river with weakly cohesive point bar cover that nevertheless developed several chute cutoffs. Therefore, in this study we added more fines and used a simple hydrograph for overbank sedimentation compared to the experimental meandering river in Van Dijk et al. (2012) with constant discharge. In this paper we test how the river sustains meandering when the bank is stabilized by a self-formed cohesive floodplain, while a floodplain without cohesion results in a braided river. We refer to self-formed cohesive floodplain as the floodplain formed by sediment deposition distributed by the water flow after the initial conditions. The unchanged initial banks are referred to as pristine plain and are non-cohesive. The area where the river changes the bed/ bank elevation is referred to reworked floodplain.

Here we show how the cohesive floodplain forms over the duration of the experiment and how this maintained a meandering channel, as well as demonstrating how the lack of cohesive floodplain led to braiding under otherwise equal conditions. To systematically evaluate bank erodibility in the experiment, tens of small-scale bank erosion tests were conducted. The objective of this study was to assess the effect of cohesive floodplain fines on; 1. the floodplain formation, 2. bank erosion and cutoff processes and 3. the channel pattern. This paper is structured as follows. First, we describe the setup and boundary conditions of the experiments, the measurement techniques, and the setup for the bank erosion tests. Second, we present results describing the bank erosion test, the detailed morphology, the water depth and the construction of the cohesive floodplain. Finally, we discuss floodplain formation and bank ero-

sion processes based on the results of the bank erosion tests and the sequence of bend development observed in the experiments.

2. Experimental setup, methods and materials

The experiments were set up to represent a gravel-bed river dominated by bedload transport (Kleinhans and Van den Berg, 2011). The designed conditions were not based on direct scaling from a particular natural river, but on an optimal reduction of scaling issues derived from a large number of pilot experiments (Van Dijk et al., 2012; Van de Lageweg et al., 2013). We designed experimental conditions that compromise between the most important scaling issues; in particular, low sediment mobility, prevention of scour holes and cohesion of the floodplain sediment. The experiments were scaled down in discharge compared to our earlier experiment (Van Dijk et al., 2012, Table 1), so that in the same length of the flume more bends could develop. Additionally, small-scale bank erosion tests were conducted to quantify the influence of silt on bank erosion rates.

2.1. Bank erodibility

2.1.1 Earlier experiments

Most experiments resulted in a braided planform by reoccupation of depressions, which form when erosion exceeds deposition (Ashmore, 1991). To obtain self-formed meanders in the lab, earlier experiments reduced the bank erosion rate by having stronger banks. A decrease in erosion rate should lead to a longer time period for sediment deposition on the inner side of the channel, so that the local differences between erosion and deposition were balanced. The earlier experiments could be divided in two different types of bank stabilization. First, several prior studies added a cohesive mixture of clay in the bed, so that inner bend floodplain formation should keep up with the outer bank erosion. These experiments led to the formation of static meanders as lateral migration ceased when the bank cohesion was too high (Friedkin, 1945; Schumm and Khan, 1972; Smith, 1998). The addition of a less cohesive silt increased bank strength of the non-cohesive bed and formed a single bend (Peakall et al., 2007). Second, others have used vegetation to add bank strength. Alfalfa (*Medicago sativa*) sprouts seeded on a braided experimental river led to local bend migration but the pattern that formed in these experiments is best characterized as wandering (Gran and Paola, 2001; Tal and Paola, 2010) rather than truly meandering. Furthermore, alfalfa sprouts increased floodplain deposition of cohesionless fines, resulting in a sustained meandering system with a moderate sinuosity (Braudrick et al., 2009).

2.1.2 Bank erosion tests

Too much bank stability decreases the dynamics of the river (Friedkin, 1945; Schumm and Khan, 1972; Smith, 1998; Gran and Paola, 2001). Therefore, we tested systematically the effect of different amounts of silt concentration on bank erosion rates. These experiments were inspired by the work of Friedkin (1945). Tens of small-scale experiments of bank retreat were conducted (Figure 1). These tests were carried out to quantitatively assess the effect of different sediment mixtures on bank erosion rates and processes. Experiments were conducted in a flume with a duct of 50 mm wide and 1 m long on a slope of 0.01 m/m and a discharge of 400 l/hr. At the end of the entrance an experimental sediment block was placed. Here the water flow attacked the bank with a sharp angle of 45° and an initial 50 mm channel width (see also Van de Lageweg et al., 2010; Kleinhans et al., 2010).

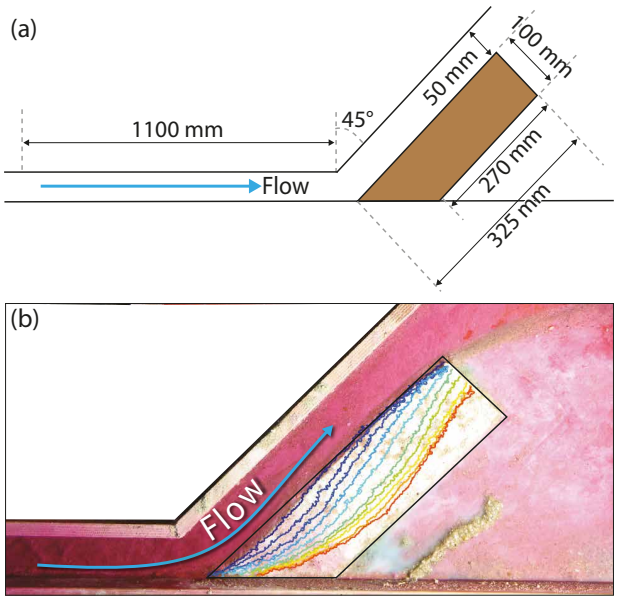

Figure 1: *Setup of the bank erosion experiment to derive erosion rates. (a) Setup of the inlet channel and the experimental sediment block. (b) Initial image of the experimental sediment block with colored lines indicating bank lines derived from subsequent images.*

Two series of bank erosion experiments were performed to test erosion rates for two different styles of floodplains: 1) The effect of sediment mixtures with different silt concentration represented continuous entrainment of sediment from the banks with lateral silt accretion and without undercutting of the bank. These banks were observed in the point bar, where overbank flow caused chute excavation. 2) The effect of a vertical-accretion of stacked silt layers on top of a non-cohesive bed was tested, which was observed in the experiment when levees, overbank

sedimentation or remnants of the crevasse were undercut by the flow at the outer bend. For the first, a floodplain consisting of different ratios between sand and silt was tested for erodibility (e.g. inner bend floodplain), where the experimental sediment block was 20 mm thick. For the other one, a floodplain was tested which had a cohesive silt drape on top of the non-cohesive sand (e.g. outer bank floodplain). Here the experimental sediment block consisted of an 8 mm, i.e. bankfull level, thick poorly sorted sand, which was draped with different thickness of silt layers.

Bank erosion rates were measured from timelapse photography of the experimental sediment block. The progress retreat of the bankline of the experimental sediment block was obtained by image processing. The bankline was used to calculate sediment area, and as thickness was known, the volume of the experimental sediment block. Data was then reduced to half-life times to characterize bank erosion rates, which is defined as the time it takes to reduce the volume of the experimental sediment block to half the initial volume.

2.2. Flume setup and experimental procedure

The experiments represented a gravel-bed river and were scaled by similarity of dimensionless variables for hydraulic conditions, sediment transport conditions and morphological features, which had to remain within specific ranges (Table 1). The flow had to be subcritical (Froude number, $Fr < 1$) as in most rivers. Turbulent flow was necessary to rework the sediment and to transport sediment in suspension in the channel and on the floodplain (Reynolds number, $Re > 2000$). For sediment transport conditions bedload sediment should be mobile $\theta > \theta_{cr}$ (Shields mobility number). A small ratio of particle size to laminar sublayer thickness is known to be conducive, so that the near-bed flow conditions affect bed scouring and ripple formation (Kleinhans et al., 2010). The channel should therefore have a hydraulically rough bed, for which large particles were needed to disrupt the laminar sublayer (grain Reynolds number, $Re^* > 11.6$). For morphological features the channel width-depth ratio determined the bar mode and bar formation, which is determined by bar wavelength and interaction parameter (Kleinhans and Van den Berg, 2011, Table 1). This required that the channels had enough bank strength, so that they did not became too wide and shallow, which ultimately leads to braiding. There are no rules for scaling bank strength, except that $\tau/\sigma > 1$ (τ is the shear strength and σ is the normal stress). Therefore, we conducted small-scale bank erosion tests to estimate sufficient conditions for erosion processes to continue, yet maintain bank stability at values higher than for cohesionless sediment.

The experiments were carried out in a flume of 6 m wide and 11 m long, which was divided into two separate plains of 3 m wide and effectively 10 m long. The flume was filled with a 100 mm thick layer of poorly sorted sand (Figure 2). The initial bed was set at a gradient of 0.01 m/m. We carved a 150 mm wide by 10 mm deep straight channel in the sediment, corresponding approximately to the predicted hydraulic geometry of a non-cohesive gravel-bed river (Parker et al., 2007) and self-formed channels in pilot experiments. The downstream boundary had a fixed weir, so that the base level was kept at a constant level. Upstream, we varied the inlet position of the sediment and water feeder with a lateral migration rate of 10 mm/hr, to mimic a bend that translates into the flume (see also Van Dijk et al., 2012).

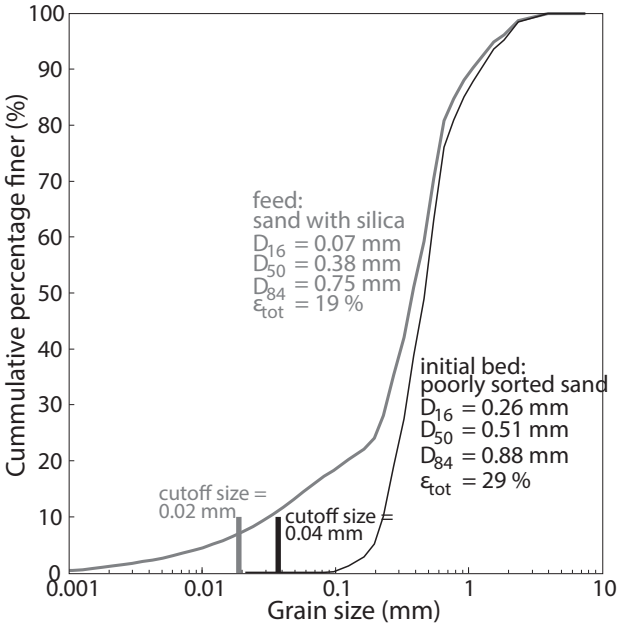

Figure 2: *Grain size distribution of the initial bed (black solid) and the feed (red dashed) sediment. The cutoff size indicates that for the sediment mixture particles smaller than 0.02 mm will percolate into the bed and that the porosity ϵ_{tot} will decrease with 10%.*

We carried out two identical experiments, which only differ in the availability of cohesive fines in the sediment feed. The addition of fines in the sediment feed represents the addition of cohesive fines to the sediment load, which led to the transition between braiding and meandering in the Rhine-Meuse delta. To one experiment we added silt-sized silica flour (D_{10}, D_{50} and D_{90} are 3.7, 32 and 97 μm, respectively) in a ratio of 1:4 in the sediment feed (Figure 2). Furthermore, an extra amount of 0.5 L silt was separately supplied during each high discharge to build a cohesive floodplain in the experiment. The Rouse number (Equation 1 Rouse, 1937) for the silt-sized fraction was smaller than 1.2, which indicates that

Table 1: *Initial and design conditions, with values for low and high discharge. We used Keulegan with $k_s = D_{90}$ ([1]), Struiksma et al. (1985, their equations 26 and 28) ([2]) and Crosato and Mosselman (2009, their equation 19) ([3]).*

Initial	Symbol	Scale rule	Value	
Median grain size	D_{50}		0.51	mm
Channel width	W		150	mm
Channel depth	h		10	mm
Valley slope	S_v		0.01	m/m
Design				
Froude no.	Fr	< 1	0.5-1.0	-
Reynolds no.	Re	> 2	$1.7 - 3.3$	$\cdot 10^3$
Shields mobility no.	θ	> 0.04	0.12	-
Shear velocity	u_*		0.03	m/s
Grain Reynolds no. [1]	Re^*	> 11.6	42	-
Bar wavelength [2]	L_p		0.9-3.2	m
Interaction Parameter [2]	IP	$0.10 < \text{IP} < 0.29$	0.12-0.47	-
Bar mode [3]	m		0.9-1.8	-
Braiding index [3]	Bi		1.0-1.4	-

the fines will transport in suspension:

$$P = \frac{w_s}{\kappa u_*} \tag{1}$$

where P is the non-dimensional Rouse number, w_s is the sediment fall velocity (in m/s), κ is the Von Kármán's constant (0.4) and u_* is the shear velocity (in m/s).

Deposition of the fine silt-sized fraction will probably not affect sediment entrainment due to changes in critical shear stress despite the reduction of median grain size. First, the addition of silt to the sand made the mixture bimodal, so that mobility differed between the two sediments and not increased mobility of the total mixture (Wilcock and Southard, 1988; Kleinhans and Van Rijn, 2002). Second, although the silt is not cohesive like clay, Lick et al. (2004) show that the critical shear stress increases for particles smaller than 50 μm. Third, fine particles will percolate into the bed (Frings et al., 2008) and calculations of the cutoff size of the sediment mixture shows that particles smaller than 20 μm (40% of the silt-sized silica flour) will neither affect bed level nor bed roughness (Figure 2, Frings et al., 2008, 2011).

A simple schematic hydrograph was used with a Q_{high} = 1800 L/hr (0.5 L/s) for 30 minutes and Q_{low} = 900 L/hr (0.25 L/s) for 2.5 hours. We ignore hysteresis of wash load supply that is often observed in natural river floods (Asselman, 1999). In the hydrograph, low flow represents approximately bankfull discharge based on the predicted hydraulic geometry in a non-cohesive gravel-bed river (W = 200 mm, h = 9 mm according to Parker et al., 2007), whereas high flow exceeds bankfull and distributed the fine sediment on the floodplain. The flood flow had an intermittency of 1:5, where 20% is flood stage and 80% of the time is bankfull stage. With constraints on the maximum discharge in the flume, the sediment had to be on average the right mobility. Furthermore, it was the duration and magnitude of low and high flow that were determined together. We designed the hydrograph to the same average discharge as in an experiment with a constant flow discharge of Q_c = 1080 L/hr (0.3 L/s), so that a volume of about 3200 L in 3 hrs flowed through both experiments. The sediment feed was kept constant at 0.2 L/hr of bedload sediment (Figure 3) during both experiments. Input discharge was controlled by a rotameter and the sediment feed was controlled by a sediment feeder. Each experiment ran for 120 hrs with one full cycle of the upstream moving boundary, with an amplitude of 300 mm in both directions.

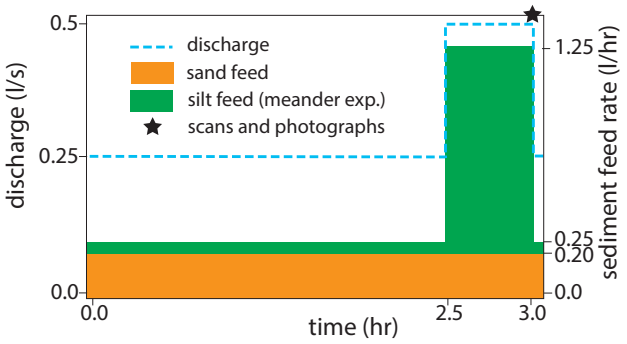

Figure 3: *Hydrograph of one low and high discharge stage with sediment feed rates. In both experiments 0.2 l/hr sand was continuously fed. In the meandering river 0.05 l/hr silt was continuously fed and during a high stage an extra 0.5 liter of silt was added. The star indicates the moment that the bed topography was scanned and photographed.*

2.3. Measurements and calibration

Several measurement techniques were used to record morphodynamics of the experimental rivers. Overhead photos were taken at a 5-min interval to create a time-lapse video of the experiment. Further, the flume was equipped with an automatic gantry, on which we mounted a high-resolution camera

(0.25 mm ground resolution) and a laser line scanner (0.2 mm vertical resolution). We measured and photographed the bed after each high discharge by pausing the experiment (Figure 3). Two LED floodlights were mounted on the automatic gantry to suppress ambient lighting. The point cloud from the line-laser was gridded on a 4-mm grid by median filtering to produce Digital Elevation Models (DEMs). The initial bed surface slope of the DEMs was subtracted to detrend the DEMs. The detrended elevation was expressed relative to the surface that remained unchanged. DEMs of difference (DoD) were calculated by subtracting DEM pairs. DoDs were thresholded by the vertical resolution (0.2 mm) of the laser line scanner.

A sediment balance was calculated by summation of the thresholded DoDs (Equation 2). The sediment balance volumes between time steps t and $t+1$ were calculated for all grid cells m based on the inversed Exner equation:

$$V_{t\rightarrow t+1} = dx \cdot dy \cdot \sum_{i=1}^{m} z_{(i,t+1)} - z_{(i,t)} \qquad (2)$$

where V is volume (in dm^3), z is bed level (in dm), dx is grid size in x-direction (in dm) and dy is grid size in y-direction (in dm), i is grid cell index and m is total number of grid cells.

To describe evolution of experiments in the flume, the total and active braiding index (TBI and ABI, Egozi and Ashmore, 2009; Bertoldi et al., 2009), the sinuosity and the distribution of the surface elevation were calculated for every time step. The water was dyed with a red color dye (Rhodamine B) to determine the channel position and water depth. The TBI, defined as the number of wetted channels per cross-section, was taken as the average number of channels (from six cross-sections at the distance of 2, 3.5, 5, 6.5, 8 and 9.5 m along the flume) identified on the DEM and high-resolution photographs where the red color band of the images corresponded to the red dyed water. The ABI, defined as the number of channels that transport sediment in a cross-section, was the average number of channels which also had net morphological change (e.g. erosion or deposition) observed on the DoD maps at the six identical cross-sections as the TBI. The frequency distribution of the detrended surface elevation (characterized by percentiles Z_5, Z_{50} and Z_{95}) was used to check whether the experiments did not aggrade or degrade, and to test if the experiment with cohesive silt developed deeper channels and higher floodplains, as compared to the experiment without cohesive silt.

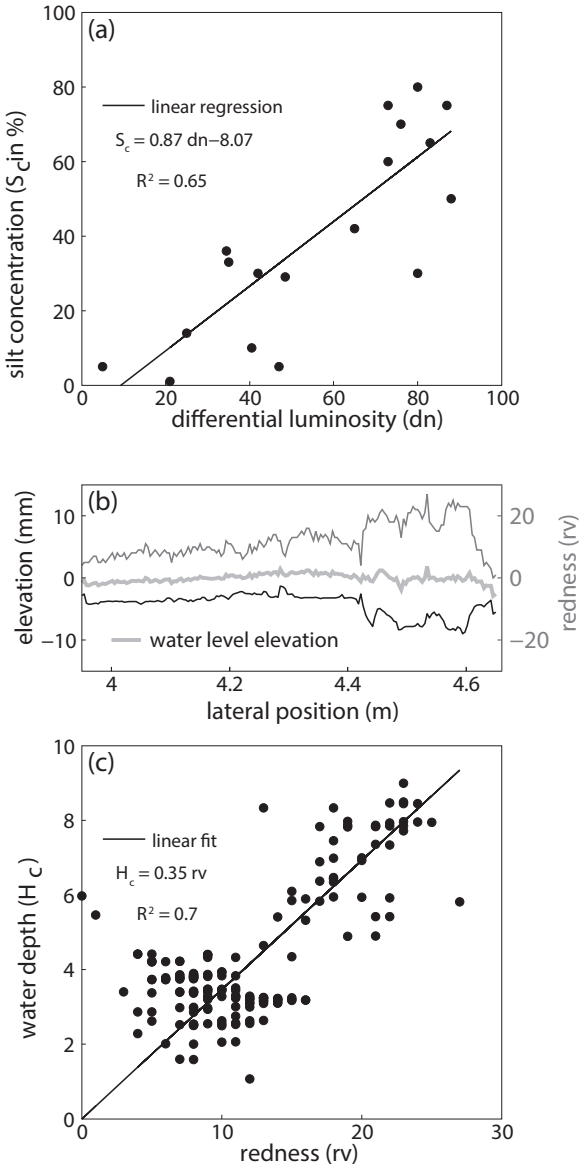

Figure 4: *Calibration dataset for silt concentrations and water depth. (a) Relation between the differential luminosity (in digital number: dn) and measured silt concentrations. (b) Downstream view of a cross-section indicating elevation and redness values (rv), which were used for the relation between the redness and water depth (H_c), given in Figure 4c.*

The high-resolution images were used to derive the concentrations of silt on the floodplain, to segment channels and to deduce water depth (based on Carbonneau et al., 2006; Tal and Paola, 2010). The high-resolution camera with RGB-band gives values for green, red and blue, which can be transformed to a $L*a*b*$ color space (CIELAB). Herein, $L*$ represents the luminosity (low = black and high = white), $a*$ is the position between red/ magenta (high values) and green (low values), and $b*$ is the position between yellow (high values) and blue (low values). The luminosity was used to make distribution maps of the highly reflective silt. Therefore, 18 samples of silt were related with the luminosity difference be-

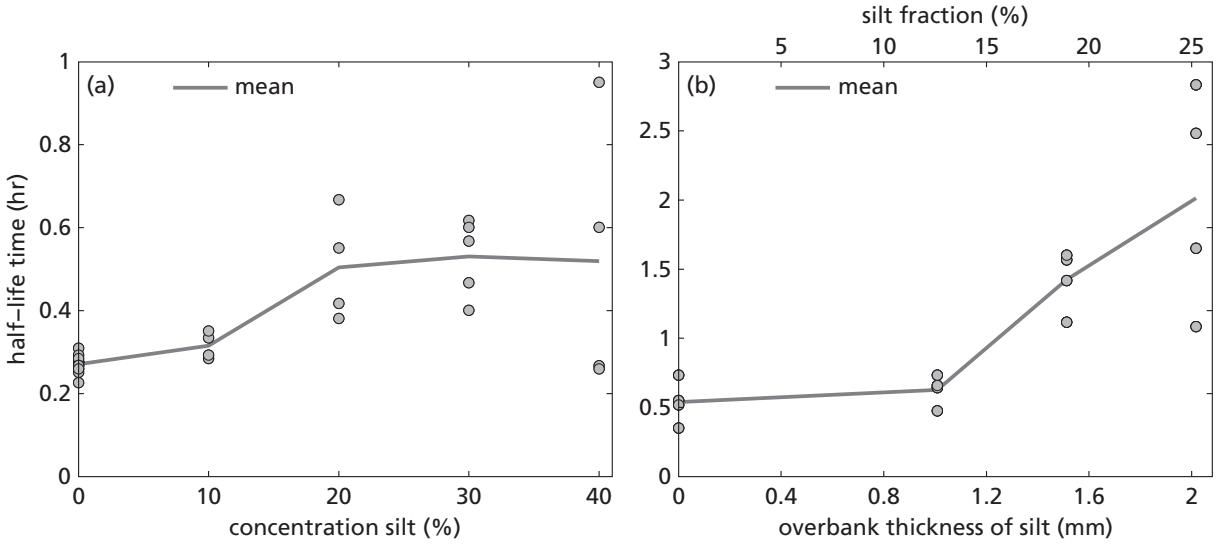

Figure 5: *Half-life times of the small-scale bank erosion experiment (after 5 cm bank erosion). (a) Well-mixed sediment mixtures. Banks became stronger with increased silt concentration representing sediment entrainment by overbank flow on the point bar. (b) Concentrations of silt on top of the poorly sorted sand. Higher silt concentrations decreased bank erosion rate as an example of lateral migration eroding a levee.*

tween the current image and the initial image of the bed (Figure 4a). The intensity of the redness ($a*$) was related to water depth for each time step, as the redness reduced during the experiment. The relation between water depth and redness intensity was found by relating the bed elevation on a cross-section with the redness intensity at that cross-section. For this relation, only points were included of the active channel and the overbank flow on the outer bank (Figure 4b-c).

3. Results

In the experiment without fines a braided river formed, while the addition of cohesive fines produced a single-thread meandering river. In this section, we describe the effect of silt on bank erosion, morphodynamics of the braided and meandering river, cohesive floodplain formation and the effect of cohesive floodplain fines on bank stabilization and chute excavation.

3.1. Auxiliary bank erosion experiments

Bank erosion experiments were conducted to quantify the effect floodplain styles with different silt concentrations on erosion rates. Initially, erosion was rapid and declined with the decrease of the experimental sediment block volume and increased channel width. Erosion of the experimental sediment blocks without a silt layer on top occurred continuously by sediment entrainment. Coarse grains of the poorly sorted sand were detached from the experimental sediment blocks. The coarse grains were not transported downstream immediately and caused local bank toe protection. A cohesive silt layer on top stuck together and was undercut resulting in the detachment of failure blocks. Silt was not directly transported and deposited at the bank toe. We suspect that silt depositing on the bank toe led to hydraulic smoother conditions and increased critical shear stresses, which caused a decrease in bank erosion. The increase of silt on top of the bank made the bank line more irregular as erosion rates differed locally. Nevertheless, the sediment mixtures eroded continuously and no failure blocks were observed. Silt fraction within the non-cohesive sands decreased the entrainment of sediment and bank erosion rates.

The addition of 20% silt decreased the bank erosion rate by a factor of 2 (Figure 5). Bank strength increased with an increase of silt concentration, until the pores were filled by silt (around 20%, Figure 5a). When the pores of the sand were filled, silt became part of the bed-structure (Frings et al., 2008). The addition of water led then to fluidazation of the silt, so that bank strength did not increase. A further increase in silt resulted in more variation of the half-life time caused by variation in compaction and a variance of the cut-off size between mixtures, so that shear stresses differ (Frings et al., 2008). The mean half-life time was the same for concentration higher than 20% silt in the mixture (Figure 5a), while lower concentrations showed no significant effect on the bank stability.

The bank strength increased when a silt layer was on top of the non-cohesive poorly sorted sand. A 1 mm thick layer of silt, about 13% of the total volume of the experimental sediment block, did not reduce the half life time (Figure 5b). An experimental sediment block with a 1.5 mm (19%) thick silt layer

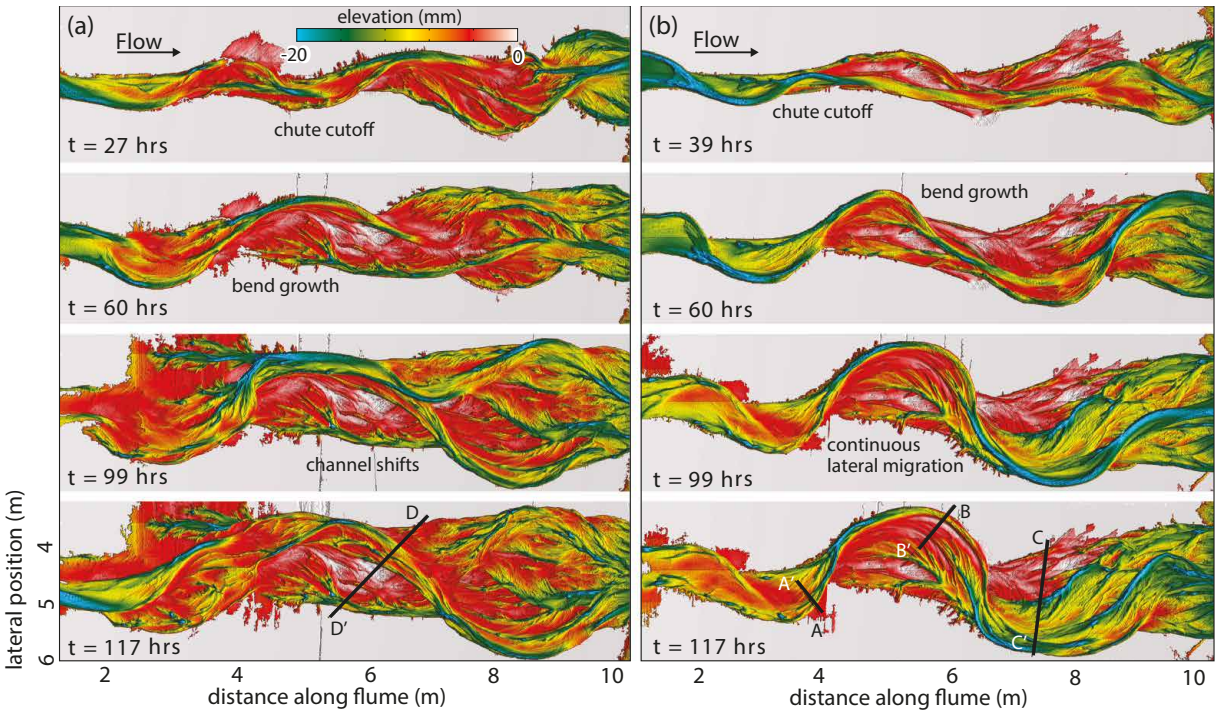

Figure 6: *Channel evolution of a braided river (a) and a meandering river (b); shaded elevation maps (DEMs) detrended with the initial slope. Unchanged surface is masked by gray. Cross-profiles are indicated for Figure 14. Scan with Layar App.*

had a much higher bank strength and reduced bank erosion almost a factor of 3. A poorly sorted experimental sediment block with a 2 mm (25%) silt layer decreased the bank erosion to a rate four times slower than without a silt layer.

3.2. Channel pattern

Our experiments resulted in a braided river as well as a meandering river (Figure 6 and Movie 1). Lateral channel migration was the dominant process in both experiments. Ultimately, meandering was sustained because the channel experienced less chute cutoffs. This was caused by the addition of cohesive fine material that deposited on the floodplain and stabilized the banks.

3.2.1 Initial alternate bars

The initial conditions for both setups were the same, so that in both experiments alternate bars formed. In this first phase, the alternate bars grew to an incipient meandering river. Thereafter, the bend wavelength increased and bends migrated in downstream direction. The most upstream bend reached the downstream bar and a chute cutoff shortened the channel in both experiments (Figure 6, 27 hrs (a) and 39 hrs (b), respectively). The incipient meandering rivers straightened and new bends formed as the upstream perturbation was maintained. The development after the cutoff of the incipient meandering river produced a braided and a meandering river. In both setups, bend formation was initiated by the upstream boundary, that continuously moved in the transverse direction.

3.2.2 Braided river

The river without cohesive fines produced a braided planform as the channel repeatedly cross-cut the self-formed floodplain. The braided river was characterized by multiple channels (Figure 7a) as indicated by the TBI, which was around 2 (Figure 8a). Nevertheless, sediment transport occurred mostly in one main channel (ABI just above 1.7). Lateral channel migration formed a point bar with typical scroll ridges and swales. Further, a subsidiary channel formed that later developed into a chute channel. After each cutoff, perturbation of the channel by the moving upstream boundary caused lateral migration, so that new bends were initiated again.

Later, continuous migration of the channel resulted in reoccupation of older channel depressions and more channels became active in the braided river (Figure 8A-B). Overbank flow was observed when the bend developed and later followed by a chute cutoff. The chute cutoff straightened the channel and lowered the water level, so that the total wetted area of the floodplain in the experiment decreased (Figure 7c). The wetted area is the area where water flows during low flow. We distinguish the total wetted area and the area that has been reworked, the difference between both is the overbank flow.

Channel adjustment and formation of bars and

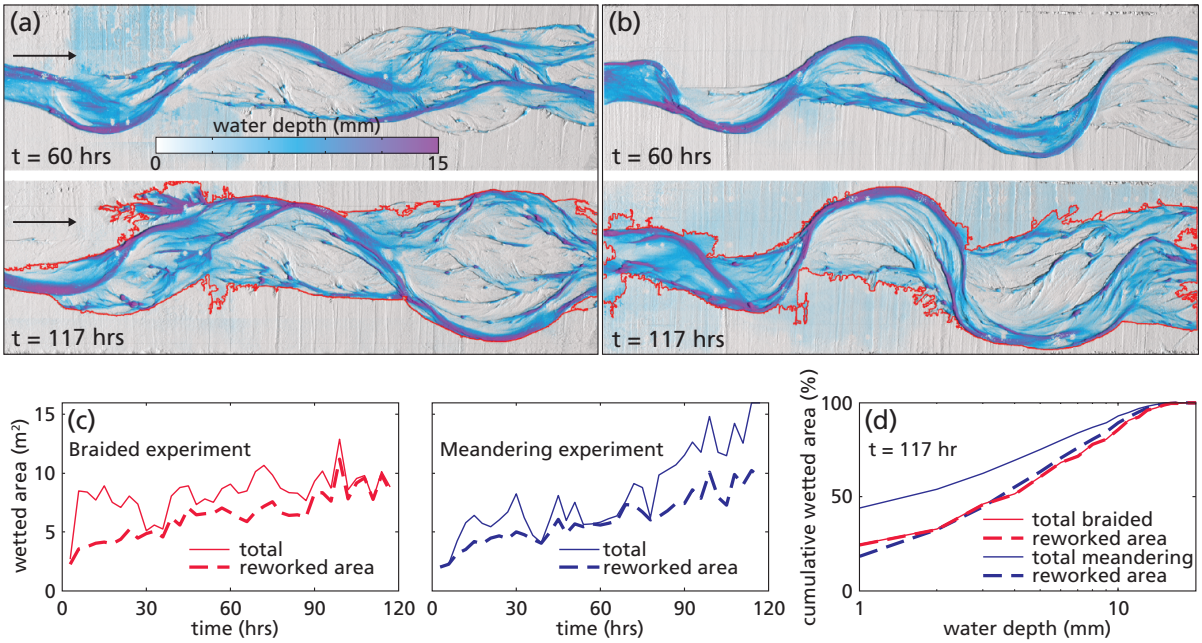

Figure 7: *Water depth maps and wetted surface area. The braided rivers (a) shows a more multi-thread system and less overbank flow for 117 hrs compared to 60 hrs, where red lines indicated morphologically changed (reworked) area. The meandering river (b) shows a more single-thread system and less overbank flow for 60 hrs compared to 117 hrs. (c) Total wetted surface area and wetted surface area for morphologically changed river and floodplain. This shows that floodplain flow declined in the braided river, while in the meandering river floodplain flow became more dominant. (d) Cumulative distribution of water depths on the wetted surface area indicates that meandering channels are slightly deeper.*

bends shaved off the floodplain. Channel extension and floodplain shaving led to sediment loss in the first 25 hrs (Figure 9b). Later, sediment loss continued as the reworked area increased (Figure 9a) and the floodplain shaved off further. As result the overbank flow in the braided declined (Figure 7c). Eventually, the total sediment balance shows a loss of 73 L, which is about 4.5 mm in height per unit area that had been reworked by the channel. Nevertheless, the channel did not incise in the floodplain as the Z_5, Z_{50} and Z_{95} of the reworked area did not change over time (Figure 9c).

3.2.3 Meandering river

The meandering river was characterized by sustained lateral migration of the channel in the middle section of the flume. The bend in the middle section of the experiment translated and expanded, so that a large bend formed (Figure 6, 117 hrs). The curvature, expansion and translation of the bend in the middle section controlled the bend downstream (e.g. migration and cutoffs). The ABI of the braided river was just above 1.5, while the ABI for the meandering river was smaller than 1.5 (Figure 8b). Eventually, sustained lateral channel migration produced a single-thread meandering river were the sinuosity increased up to 1.4 (Figure 8b, c).

The meandering river developed after the cutoff of the incipient meandering river. In the initial channel alternate bars developed, which increased the sinuosity and roughness of the channel. When the bend became sharper water level rose and overbank (floodplain) flow occurred even during low flow, so that for example the total wetted area was larger than the wetted area of reworked floodplain, while in the braided river they became equal (Figure 7c). Concentrated overbank flow resulted in a chute cutoff of the non-cohesive incipient meandering river and decreased the wetted area as the channel straightened (Figure 6, 39 hrs). The upstream moving boundary triggered lateral migration of the bend and the eroded sediment deposited upstream of the chute channel and formed a plug bar (Figure 6, 60 hrs). Later, the bend extended and translated, which resulted in a continuous increase of the bend amplitude and bend length (Figure 6, 99 hrs). Eventually, a large bend developed in the middle section of the flume with a typical scroll ridge-swale topography (Figure 6, 117 hrs). The bend was not cross-cut even when the upstream moving boundary moved in reverse direction seen in Van Dijk et al. (2012).

In the meandering river fines settled on the floodplain when water level exceeded bankfull elevation. Overbank flow on the pristine plain occurred when the bends became sharper in the meandering river, but also for the incipient meandering river in both experiments (Figure 7c). The wetted area without overbank flow on the pristine plain was equal for the braided and the meandering river (Figure 7c). Overbank flow in the meandering river resulted in a large area

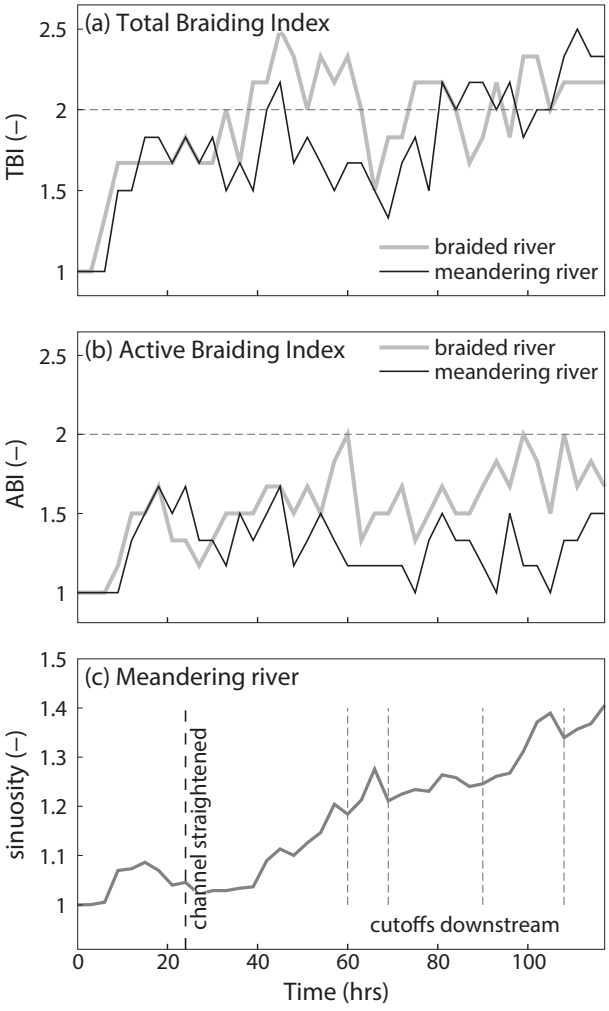

Figure 8: *Channel pattern descriptors. a) Total Braiding Index (TBI) for the braided and meandering river. b) Active Braiding Index (ABI) for the braided and meandering river. c) Sinuosity of the meandering river, with a cut-off of the incipient meandering river after 30 hrs and small chute cutoffs of the downstream bend.*

of shallow water depth at the end of the experiment (Figure 7d). The water depth distribution without pristine overbank flow and the surface elevation at the end (Figure 9d) showed that the channels were slightly deeper and the floodplain slightly higher for the meandering river. Channels in the braided river were less deep as water was divided over multiple branches (Figure 6, 117 hrs).

As in the braided river, channel adjustments and rapid migration of the bends resulted in sediment loss over the first 20 hrs (Figure 9b). The meandering river reworked a smaller area and the absolute sediment loss was also less (Figure 9a-b). Overall, the sediment loss was 4.9 mm in height over the reworked area compared to 4.5 mm in height for the braided river. A reason for this difference could be that the channels in the braided river were less deep and the floodplain shaving effect was smaller.

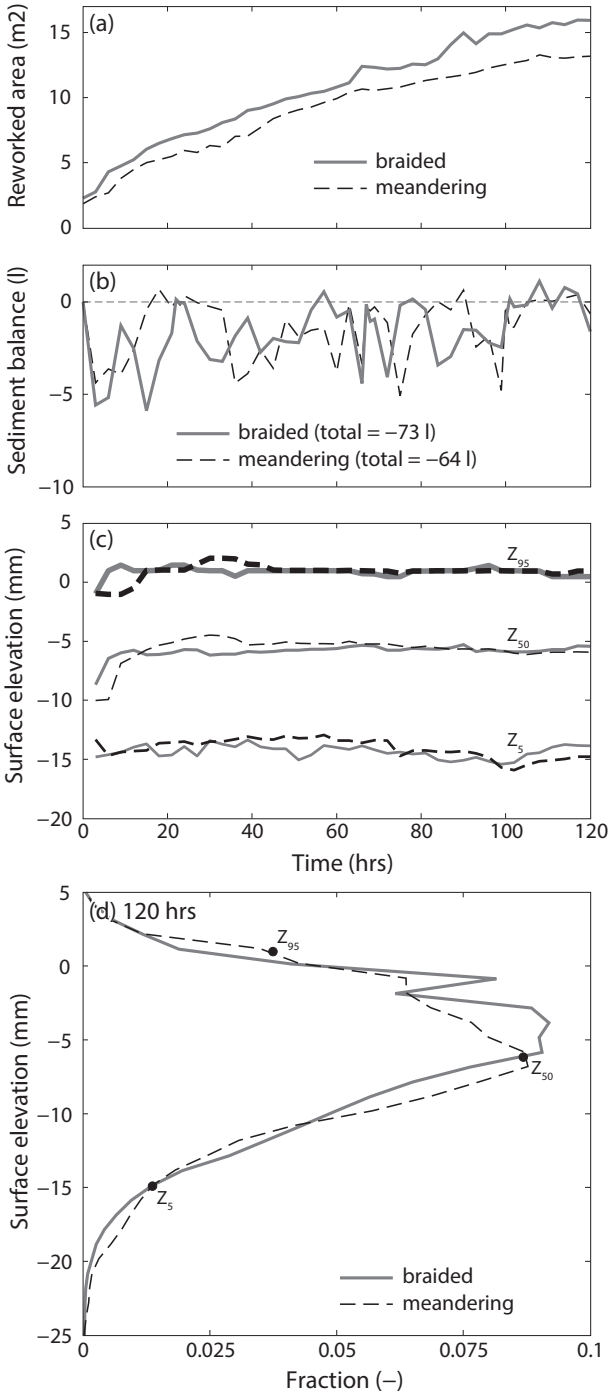

Figure 9: *Descriptive statistics of the flume experiments. (a) Time series of the reworked area. (b) The sediment balance shows sediment loss when the reworked area increases. (c) Time series of the detrended median surface elevation and of the spatially-averaged range of detrended surface elevations of the reworked experimental surface. The surface elevation shows that the 5^{th} remains the same which indicates that no incision occurred for both experiments. (d) Probability distribution of detrended channel belt surface elevation at the end of the flume experiments. Dots indicate percentiles plotted in (c).*

Although the sediment loss was higher, the surface

elevation did not show more degradation (Figure 9c). The Z_5, related to the deepest part of the reworked area, did not became lower, i.e. deeper. At the end of the experiment, the surface elevation illustrated that the meandering river, as compared to the braided river had deeper (Z_5) and shallower points (Z_{95}) in the reworked area, i.e. the meandering river had both a deeper channel and a higher floodplain (Figure 9d).

3.3. Floodplain deposition and styles

The floodplain was formed by deposition and erosion of sand and silt and by enrichment of silt during overbank flow. Two characteristic floodplain styles were observed by the deposition of cohesive silt. The first style was formed by deposition of silt on the outer bank (vertical-accretion), such as crevasse splays, levees and overbank sheets of silt deposits. The second style was found on the inner bend (lateral accretion), where silt deposited during lateral migration and later on the point bar scrolls and in the lower swales (overview in Figure 10a).

3.3.1 Silt distribution

Silt deposited in different styles on the meandering river and was not uniformly distributed along the meandering river. Continued silt addition resulted in an increase in the surface area fraction containing silt and an increase in silt concentrations over time (Figure 10b). Low concentrations of silt settled along the main channel during the formation of the incipient meandering river (Figure 10c). Later, the highest silt concentrations were observed near the flume inlet as overbank flow occurred on a small area, while silt concentrations in the water were relatively high, causing deposition. In the middle section, a large bend developed and captured most of the silt. Continued deposition of silt increased the silt concentration in the middle section (Figure 10c-d). Deposition of the silt led to depletion of the silt concentration, so that the surface fraction area of silt and concentration decreased in the downstream direction. After the incipient meandering river was cutoff, silt was removed by channel migration without depositing a new layer of silt in the downstream section.

3.3.2 Inner bend deposits

Point bars developed as the channel migrated laterally and sediment deposited on the inner side of the bend forming scroll bars, while sheet flow over the point bar resulted in lobate bars. Silt deposited on the lee sides of the point bar, i.e. swales, by overtopping the scroll and lobate bars and depositing along the main channel (Figure 11a).

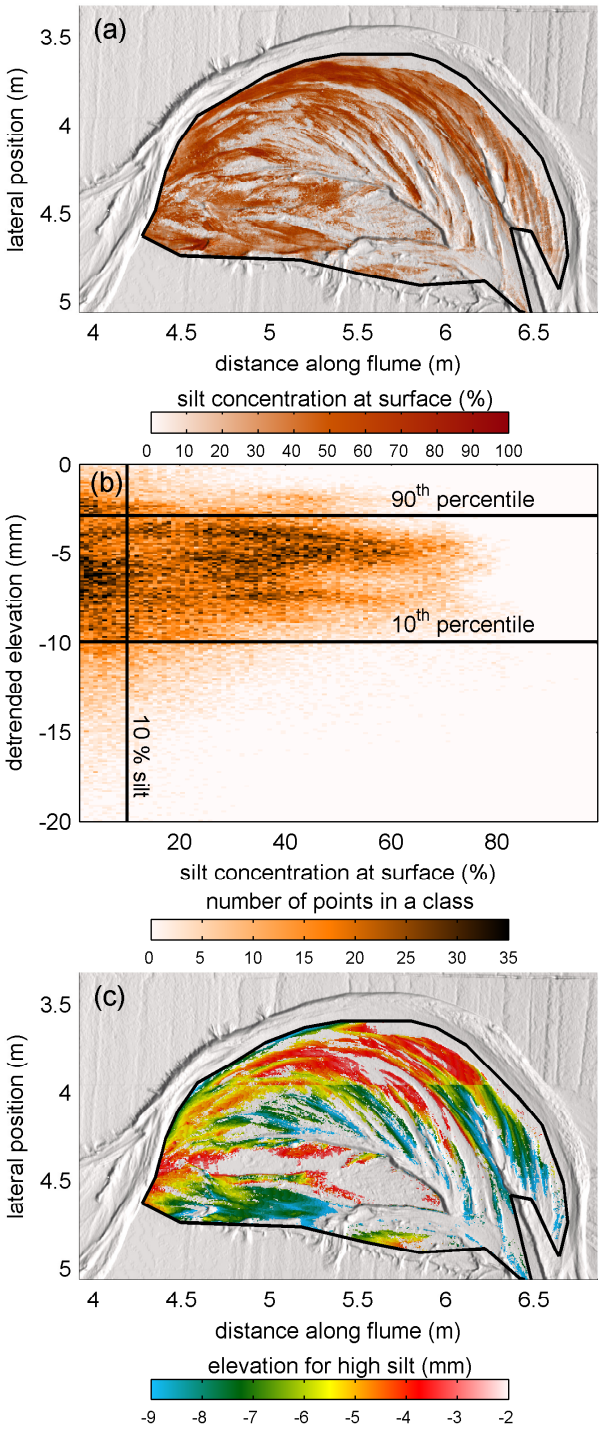

Figure 11: *Silt deposition on the point bar. (a) Silt map at t = 117 hrs. (b) 2D histogram of the detrended elevation and silt concentrations, the lines indicate the 10^{th} (-9.9 mm) and 90^{th} (-2.9 mm) percentile. Silt concentration peaks are found around elevations of -7.4 mm, -5.4 mm and -3.9 mm (purple). (c) Elevation map of silt on the point bar, where the peaks are visible by green, yellow and red.*

Silt was spread on various elevations of the point bar; in the low swales, in a subsidiary channel and on the higher scrolls. Most of the silt deposited between the detrended elevation of -2.9 and -9.9 mm and the highest concentrations were clustered at detrended elevations of -7.4, -5.4 and -3.9 mm (Figure 11b). The

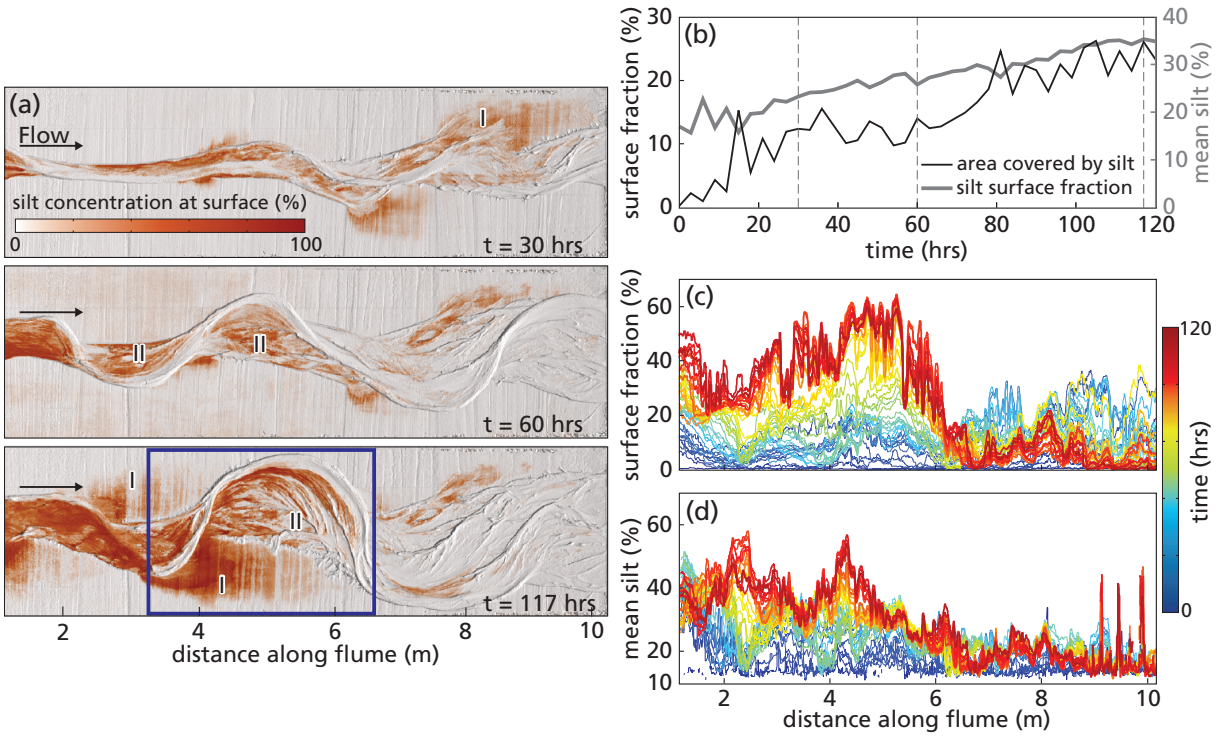

Figure 10: *Floodplain surface fraction with a silt fraction of more than 10% along the flume in the meandering river. (a) Surface deposition silt after 30, 60 and 117 hrs. Box indicates the area of interest for Table 2, and I and II indicate floodplain styles. (b) Time series of area with more than 10% silt at the surface and the silt concentration averaged over the surface area. (c) Width average silt fraction of the surface along the flume shows that most silt is captured upstream. Note erosion of silt downstream of the large meander. (d) Average silt concentration for grid cells with at least 10% silt. Note that the highest silt concentrations were found in the upstream section of the flume.*

lowest elevation of silt on the surface (-7.4 mm) was located in the most downstream part of the swales and in the remnants of the chute (subsidiary) channel (Figure 11c, blue). The chute channel was abandoned due to a plug bar upstream, while downstream silt deposited without filling the channel remnants. Silt on the surface (-5.4 mm) deposited also on the upstream part of the swales and on the scrolls along the channel (Figure 11c, yellow). The highest elevation of silt on the surface (-3.9 mm) was located on the chute bar formed during the incipient meandering river and on the active scrolls (Figure 11c, red). The lowest areas were not entirely filled with silt, so that depressions such as chutes and swales remained visible.

3.3.3 Outer bank deposits

The sharper bends in the meandering river promoted overbank flow on the outer bank, which caused formation of crevasse splays and levees. Downstream of the sharpest part of the bend, a high-momentum flow advected onto and over the point bar in the curved channel, so that overbank flow occurred and diverted on to the pristine plain. The interaction between flow strength and bank strength resulted in crevasse splays or levees, respectively. Crevasse splays or levees did not form in the braided river as flow curvature was generally low, so that water level did not rise above the pristine plain (Figure 7c).

The crevasse channel with splay formed during the incipient meandering phase when the banks were not yet cohesive. Downstream of the crevasse channel, a sandy splay formed with silt deposits at the lee side (Figure 12a). Later, the upstream bend migrated in lateral and downstream direction and the flow direction in the crevasse became more perpendicular to the channel. The former crevasse channel was abandoned and filled with fines, while in the new crevasse channel silt deposited again at the lee side of the crevasse splay (Figure 12b). Eventually, a chute cutoff in the main channel shifted the flow direction, so that the crevasse was abandoned. The remnant of the crevasse splay was partly filled with silt by overbank flow occurring on the crevasse splay (Figure 12c).

In the meandering river, continuous overbank flow with silt on the pristine plain led to formation of a levee. The banks were stronger, so that sediment deposited on the outer bank instead of channel incision and the formation of a crevasse. The thickness and location of the levee depended on the occurrence and direction of the overbank flow. Overbank flow followed the initial slope and spread outwards from the sharpest point of the bend (Figure 13a). In

planform view, the overbank deposit formed a splay shape, that was interrupted due to the low ridges on the initial pristine plain (Figure 13a). On these ridges, the silt fraction decreased as water depth decreased and apparently flow velocity increased (Figure 13b).

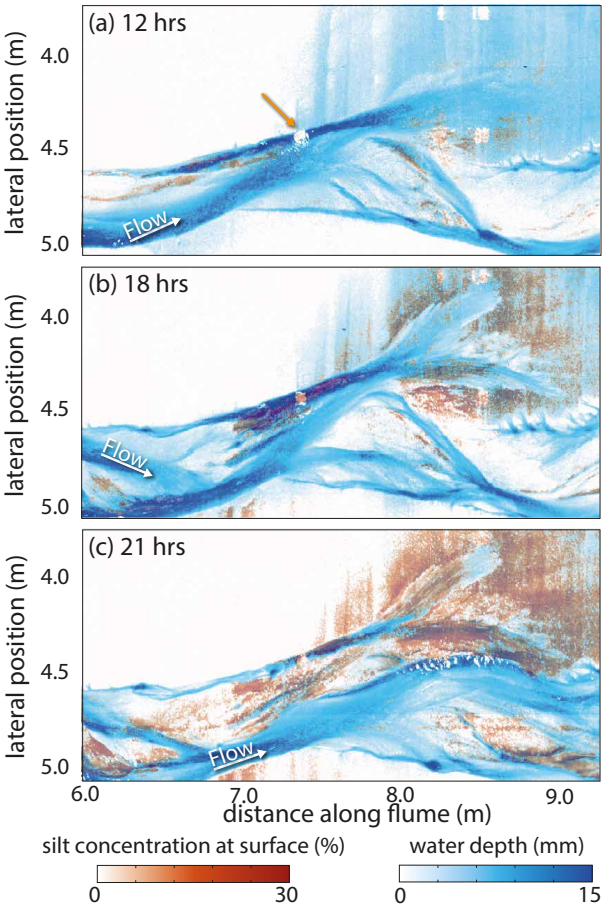

Figure 12: *Crevasse splay development and associated silt distribution. Initially, silt deposits downstream of the crevasse splay (a), but when the channel was abandoned, the splay was filled with silt (b and c). White spots (indicated by orange arrow) were caused by the light reflection on the water surface.*

Deposition of sand and silt raised the floodplain elevation. Near the channel, sand deposition was dominant compared to silt deposition. The deposited sand fraction raised the floodplain elevation by 2 mm (Figure 13b). Spreading of the overbank flow resulted in deposition of more silt and less sand in downwards direction. The concentration of silt deposits varied in longitudinal and lateral direction. First, in longitudinal direction the percentage of the area covered by silt increased, but further downstream percentage of silt decreased as most silt was already deposited (Figure 13b). Second, the percentage of silt was non-uniformly distributed in lateral direction (Figure 13c). High concentrations of silt raised the floodplain elevation by 0.5 to 1.5 mm (Figure 13b-c).

3.4. Bank stabilization

In this section, the relation between bank erosion and floodplain style is explored. First, the floodplain area that stabilized the banks is described. Second, bank erosion is related to meander migration in several bends.

3.4.1 Bank stabilization by floodplain construction

In the meandering river, several floodplain styles formed and stabilized the banks. These floodplain styles were eroded by different processes, i.e. bank undercutting or sediment entrainment (Table 2). The self-formed floodplain reduced bank erosion upstream, chute incision and headcut formation downstream of the point bar, so that the meander bend was not cut off (as in Van Dijk et al., 2012). At the meander bend in the middle section, a total area of 7.9 m^2 (see Figure 10), several cohesive floodplain styles developed and covered about 40% of the area. On the pristine plain (total area of 4.3 m^2) silt covered an area of 1.75 m^2, which was 41% of the total pristine plain area and was mostly concentrated on one side of the channel (Table 2). On the inner bend (total area of 3.6 m^2) 43% of the area was covered by silt. Here, silt deposited during lateral accretion and during overbank flow on the higher scrolls (1.0 m^2) and in the lower swales (0.5 m^2). The bank erosion test demonstrated that addition of silt in the floodplain reduced erosion rates.

Table 2: *The surface area with floodplain formation styles occurring in relation to floodplain removal by bank undercutting and chute incision in the middle section of the meandering river (see Figure 10a).*

floodplain style	area	undercutting	incision
total area	7.9 m^2		
overbank area (I)	4.3 m^2		
crevasse	0.0 m^2	X	-
pristine	1.8 m^2	X	-
inner bend area (II)	3.6 m^2		
ridges	1.0 m^2	X	X
swales	0.5 m^2	-	X

3.4.2 Bank erosion in channel experiments

Table 3: *Channel displacement (migration rate) related to cohesive silt deposits (bank properties) and the sharpness of the bend (curvature) for cross-profiles A-C from 57-117 hrs (Figure 14).*

Profile	Bank properties	Curvature (R/W)	Migration rate (mm/hr)
A	layered	5.2	4
B	top cohesive	11.2	12
C	non-cohesive	13.1	5

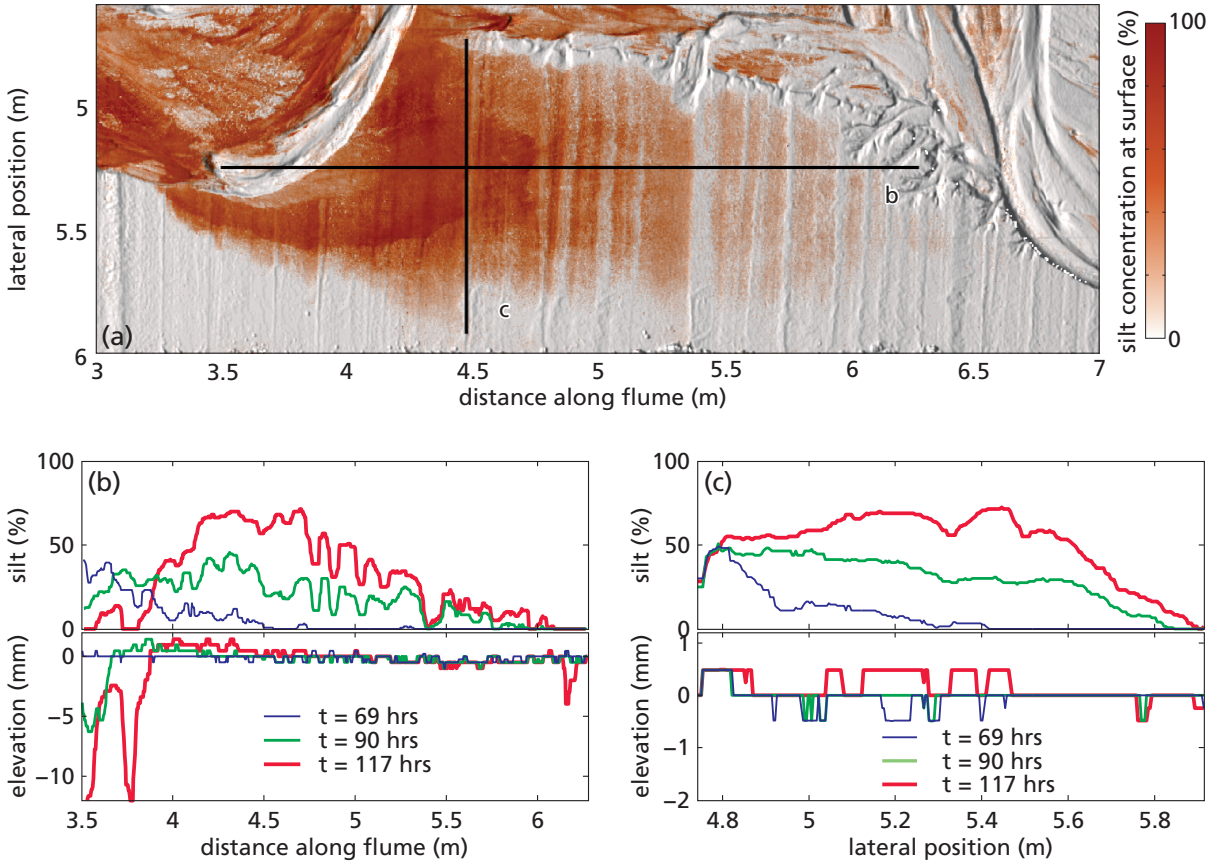

Figure 13: *Floodplain sedimentation of silt on the outer bank forming a levee. (a) Silt map with indicated profiles b and c. (b) Longitudinal distribution of silt. Sedimentation of sand and silt increased the bed elevation on the pristine plain. (c) Transverse distribution of silt.*

Distinct floodplain styles and bank erosion processes resulted in differences in channel bend displacement in our experimental setup. Here we describe the migration of four bends (for location of cross-profiles see Figure 6). Three bends formed in the meandering river, where silt concentration around the bends decreased in the downstream direction (Figure 10). The first bend was characterized by silt deposition on the inner side of the bend and on the outer bank. The second bend had dominantly silt deposition on the inner side of the bend. At the third bend some silt deposition occurred on the outer and inner bend. Also, one bend was analyzed from the braided river, representing a bend without any effect of a cohesive floodplain.

In the upstream bend, deposition of silt on the outer bank resulted in the formation of a levee and an increase in bank strength. In the experiment, channel migration rate decreased despite the sharper bend curvature over time (Table 3). Because deposition of silt continued, chute excavation decreased on the inner side of the bend (Figure 14a). The migration rate of the bend in the middle section was faster despite the gentle bend (Table 3). Here, bank strength was not increased by silt deposits on the outer bank (Figure 14b). Consequently, there was less time for silt deposition on the inner side and the concentration was therefore lower. Cross-profile B shows that silt deposition occurred mainly in the lows of the point bar, which halted chute incision.

Reoccupation or excavation of channel depression remnants occurred more often where silt had hardly deposited. The downstream bend of the meandering river had some small chute cutoffs on the active point bar. The first chute cutoff occurred after 57 hours due to a flow direction shift caused by a bar upstream of cross-profile C. Later, upstream meander growth caused a local avulsion of the main channel as remnants of the former channel were reoccupied. Outer bank resistance by silt deepened the channel (Figure 14c). The second chute cutoff occurred on the active point bar, which was caused by the upstream bend that translated downstream and shortened the flow path. Remnants of the crevasse splay were not reoccupied as silt deposits stabilized the floodplain surface, preventing incision of chute channels (left side of the cross-profile C). Due to chute cutoffs, the average migration rate of the bend was lower, despite low silt concentrations on the outer bank and a bend curvature comparable to that in cross-profile B (Table 3).

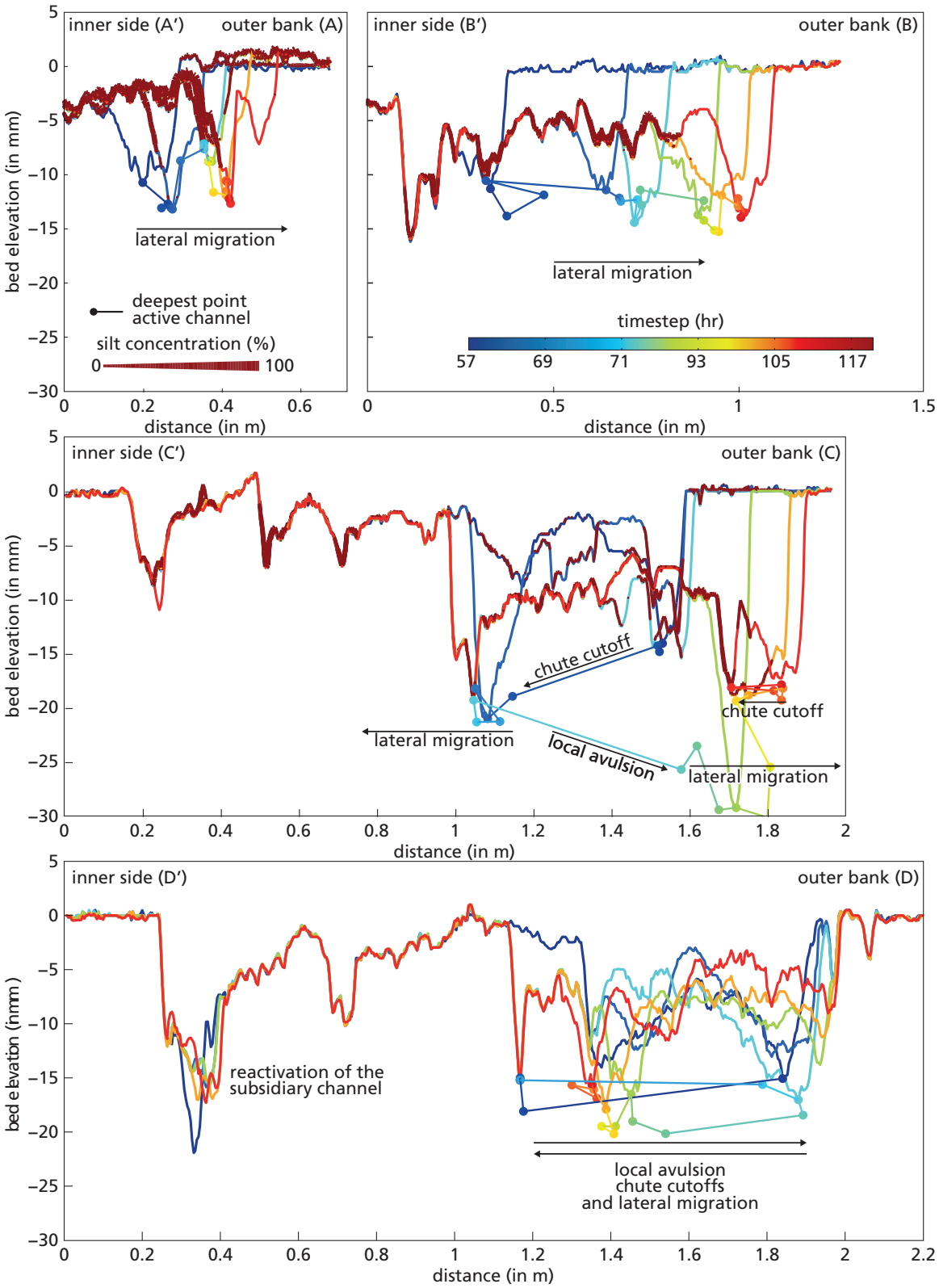

Figure 14: *Evolution of several bends, for the meandering (A,B and C) and braided experiment (D) (see Figure 6). (a) Small bend amplitude with a high concentration of silt reduced outer bank erosion and lateral migration, while it stabilized the inner bend. (b) Silt stabilized the lows, while the channel migrated laterally. (c) Less silt resulted in reactivation of lows and chute cutoffs downstream of the large meander. (d) In the braided river, the amplitude of the bend formed by lateral migration decreased due to local avulsion of the channel that shifted the flow direction. Silt concentrations are given by the thickness of the brownish line, cross-profiles and deepest points of the active channel (dots) are colored for each time step.*

Local avulsions and chute cutoffs were more common in the experiment without fines. The main channel was located for most of the time at the outer bank, but local avulsions and chute cutoffs limited the bend growth (Figure 14d). Flow direction shifted continuously reoccupied channel remnants as the floodplain consisted only of erodible non-cohesive sediments (Figure 5). Here, the subsidiary channel was excavated by overbank flow on the point bar, but it did not become the main channel (Figure 14d). The cohesive floodplains on the outer bank reduced outer bank erosion and thus lateral migration, while the cohesive floodplain in the inner bend decreased channel incision and headcut formation.

4. Discussion

4.1. Channel pattern and scaled conditions

Our experimental results demonstrate the development of a braided and meandering river. Cohesive fines deposited in the floodplain stabilized banks and led to a sustained meandering river. In the braided river, one or two channels remained active most of the time (ABI above 1.7). As observed in other studies on braided rivers in the flume (e.g. Ashmore, 2001; Egozi and Ashmore, 2009), continuous cross-cutting of the channel on the floodplain resulted in extensive shifting of the channel and bars. Field studies (e.g Reinfeld and Nanson, 1993) have described braided river evolution by lateral migration of a braid-train, but this kind of braiding did not develop in this experiment. Lateral channel migration is the dominant process in the braided and meandering river as the channel belt increases (Van de Lageweg et al., 2013). Later, cutoffs in the braided river decreased lateral channel migration.

In this experiment a cohesive silt was added for bank stabilization. In earlier experimental work, bank stabilization was accomplished by manual addition of vegetation on the floodplain (Tal and Paola, 2010). Braudrick et al. (2009) added low-density material behaving as fine sediment, which was captured by the vegetation and filled potential chutes, so that single-thread meandering was sustained. Other studies (Friedkin, 1945; Schumm and Khan, 1972; Smith, 1998) tested the effect of initial cohesive banks on meandering river development. Bank stabilization should decrease lateral migration, so that sedimentation on the inner bend increases to original floodplain level. In an earlier experiment (Van Dijk et al., 2012) a large chute cutoff reset the development of the meander bend after the upstream perturbation moved in reverse direction and restarted new bend development. Here we show that the addition of even more silt prevented cut off even after reversed movement of the upstream boundary. Our results indicate sustained meandering forms when there is a self-formed cohesive floodplain without manual interference as required in the case of seeding vegetation.

Our results showed the difference in channel development between experiments in which the only condition that was varied was the availability of cohesive fine material in the sediment feed. In an earlier experiment with less silt and a constant discharge, floodplain formation was limited and chute cutoffs could occur (Figure 15a, Van Dijk et al., 2012). A downscaled experiment with constant discharge (0.3 l/s) shows that overbank flow was limited and bends became shorter (Figure 15b). The lack of overbank flow supports the idea of the importance of a varying discharge for the formation of a cohesive floodplain (Figure 15c-d). Another effect of the varying discharge is that the wavelength of the bend increases due to the effectiveness of sediment transport during high discharges (Figure 15b versus Figure 15c,). We observed that for the low discharge and shallow channels average sediment mobility decreases, so that when flow dispersed over the floodplain the morphological changes reduced.

4.2. Bank erosion and chute cutoffs

The bank erosion experiments show that the addition of slightly cohesive silt decreases bank erosion and increases bank stability. The erosion rate can be quantified using an excess shear stress formula in which bank erosion is related to flow shear stress, critical shear stress and an erodibility coefficient (e.g. Rinaldi and Darby, 2008; Darby et al., 2010). With the bank erosion experiments we tested the erodibility coefficient of the sediment mixtures. However, prediction of the critical shear stress for cohesive material is complex as for cohesive sediments the fluvial entrainment threshold increases (Zanke, 2003; Lick et al., 2004; Rinaldi and Darby, 2008). We suspect that an increase of silt in the sediment mixture at the bank toe causes hydraulically smooth conditions and increases the critical shear stress for sediment entrainment as the sand is protected against turbulence by a viscous sublayer (e.g. Zanke, 2003; Vollmer and Kleinhans, 2007), both of which effects cause a decrease in bank erosion.

Silt on the bank toe originating from the bank top reduced bank erosion in the experiment. Deposition of silt on the outer banks forms a layer of cohesive silt on top of a non-cohesive bank. The erodibility of the non-cohesive sand is higher, so that flow undercuts the cohesive silt and failure processes with bank toe protection determine bank erosion rates, as in natural rivers with cohesive banks (e.g. Simon and Collinson, 2002; Darby et al., 2007; Langendoen and Simon, 2008; Parker et al., 2011).

Floods enhanced the occurrence of chute cutoffs by bank incision and excavating floodplain depres-

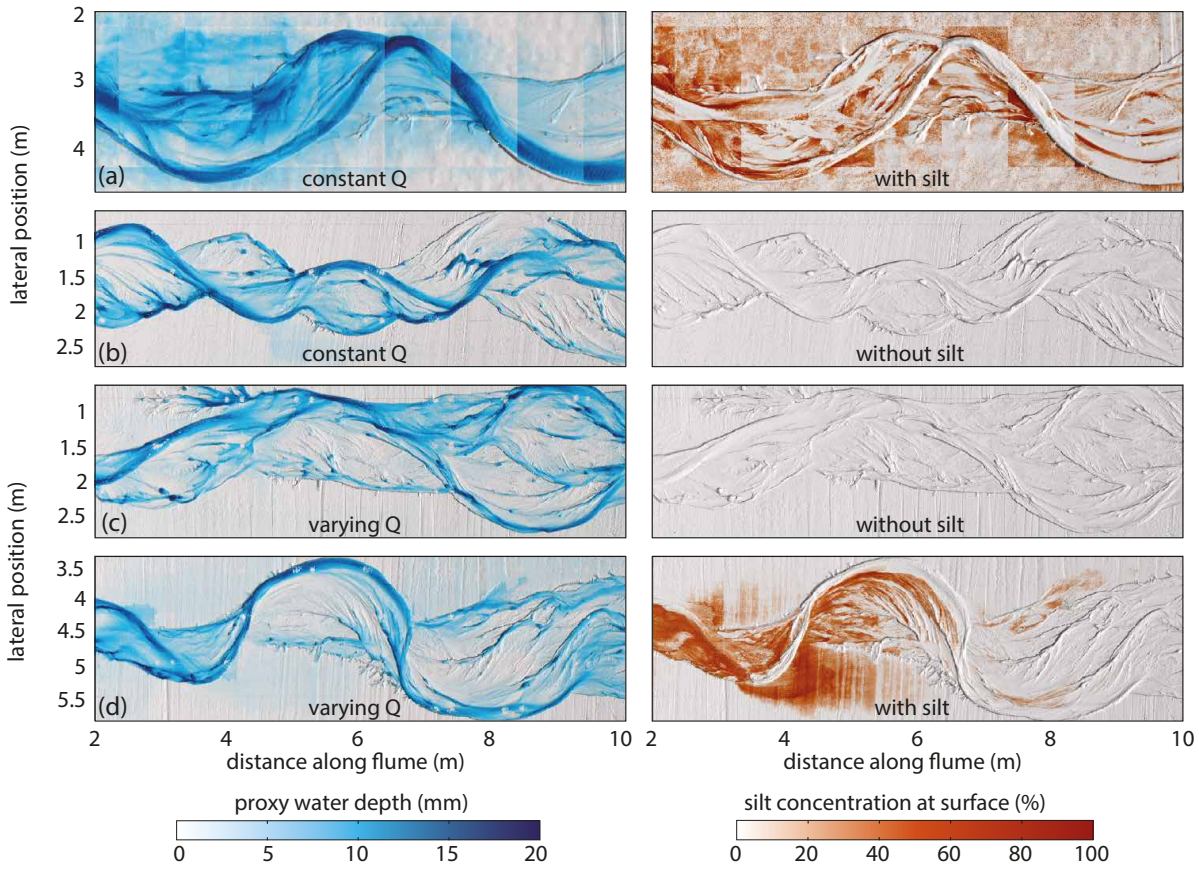

Figure 15: *Water depth and silt concentration maps for several experiments. (a) Experiment with a constant discharge (1 l/s) with silt addition. No clear development of a cohesive floodplain (t = 142 hrs). (b) Experiment with a constant discharge (0.3 l/s) without silt. Bends were shorter and overbank flow decreased over time (t = 114 hrs). (c) Experiment with varying discharge and without silt. The bar wavelength increased compared to constant discharge and a larger area was reworked at t = 114 hrs. (d) Experiment with varying discharge and with silt addition. A large bend developed, while a cohesive floodplain formed and stabilized the banks (t = 114 hrs).*

sions. Channel migration causes a local imbalance of more erosion compared to deposition and forms depressions (Lauer and Parker, 2008). Without bank stability, these depressions are captured by chute cutoffs causing the channel to braid. Chute cutoffs formed by upstream bank incision and downstream headcut formation in the point bar lows (Constantine et al., 2010; Zinger et al., 2011; Van Dijk et al., 2012). In the meandering river, the erosion processes were balanced by the cohesiveness of the fines reducing bank erosion and chute excavation. In the experiment without fines, the local imbalance between erosion and deposition was not compensated with stronger banks so that chute cutoffs cause the channel to braid. Silt depletion in the meandering experiment decreased cohesive floodplain formation and increased chute incisions and cutoffs in the downstream section.

4.3. Floodplain sedimentation

Overbank flow is required for floodplain formation (e.g. Lewin, 1978; Nanson and Croke, 1992; Zwolinski, 1992). Overbank sedimentation is enhanced by several factors, e.g. river slope, lateral channel movement, baselevel and the occurrence and magnitude of floods (Zwolinski, 1992). In our experimental setup we used a simple hydrograph, with a long period low flow representing bankfull discharge and a short period of high flow representing a flood. During the high flow period, sedimentation of the fine material on the banks decreased the local sediment imbalance between erosion and deposition (Lauer and Parker, 2008). Furthermore, the floodplain with silt became more cohesive. Overbank sedimentation of fines causes two styles of floodplain formation; in the outer bank forming levees and crevasse splays and in the inner bend in chutes and between and on scroll ridges and swales.

The floodplain in the experimental meandering river was similar to floodplains found in natural river systems. The deposition of fines on the outer bank forms a levee with coarse grains near the channel and finer, but also thinner, deposits further away from the channel (e.g. Brierley et al., 1997; Walling and He, 1997; Ferguson and Brierley, 1999). Natural levees form along the channel when water level exceeds bankfull levels. Here, the levee formed only at

the outer banks downstream of the bend apex when overbank flow spread outwards and contains fine material. The formation of a crevasse on the outer bank formed when the flow strength was stronger than the bank strength, as described for natural systems (O'Brien and Wells, 1986; Bristow et al., 1999). Fines settled on the distal side of the crevasse splay as observed in the Brahmaputra and the Cumberland Marshes (e.g. Coleman, 1969; Pérez-Arlucea and Smith, 1999). Later, the crevasse splay was abandoned by the main flow and fine silt particles buried the crevasse channel, as formed in aggrading rivers with suspended fine material (e.g. the Colombia River, Makaske, 2001). An important process in the construction of the distal levee and crevasse splay was advective deposition of the suspended material (Cazanacli and Smith, 1998) rather than diffusive mechanisms (Törnqvist and Bridge, 2002). The advective process was more important in the experiment as the floodplain flow was not turbulent, while in natural systems the effect of turbulence results in a stronger decrease in thickness and grain-size in the levee (Törnqvist and Bridge, 2002).

Silt deposition affected meander formation mostly in the middle section of the meandering river. In the upstream reach extensive silt deposition decreased bank erosion and the bend amplitude, which caused a lower bend amplitude, whereas downstream silt deposition was supply-limited which allowed the development of chute cutoffs on the point bar. We hypothesize that depletion of silt deposition in the downstream section would become less when the initial bed of a sediment mixture consists of at most 10% silt, which would not affect bank stability as shown in the bank erosion experiments.

4.4. Relevance for natural rivers

The experimental results support earlier ideas that bank strength is a necessary condition and a key parameter for river meandering (Ferguson, 1987; Eaton, 2006; Kleinhans, 2010; Kleinhans and Van den Berg, 2011). Cohesive outer banks will reduce lateral migration and decrease channel dynamics. More important is that the self-formed floodplain prevented chute cutoffs. To form a cohesive floodplain discharge variation is important because it allows fines to settle on higher banks (Middelkoop and Asselman, 1998). In nature, levees form and cohesive banks when water level fluctuates (Brierley et al., 1997).

This experiment suggests that the *initial* plain does not need to be cohesive. When the initial bed is non-cohesive, alternate bar formation and bend migration occur rapidly. The supply of cohesive material entering from the hinterland, our upstream boundary, could stabilize the banks. For example, the addition of cohesive fines to the sediment load of rivers at the transition of a glacial to interglacial climate could stabilize banks, decrease cutoffs and could cause the transition between braiding and meandering, as observed in the Rhine-Meuse delta (e.g. Vandenberghe, 2003; Erkens et al., 2011). Meandering patterns as present in the middle and late Holocene may have formed rapidly in the early Holocene, but were fixated when the amount of cohesive material on the floodplain increased whilst gradient reduced due to base level rise. Rivers with less cohesive material in the sediment load are more dynamic and have more cutoffs, such as the River Allier in France and the River Rhine at the apex of the delta around the border of the Netherlands and Germany.

Several studies ascribe the transition between braided and meandering to the vegetation cover in the river plain, which is largely controlled by climate conditions (e.g. Millar, 2000; Gibling and Davies, 2012). Vegetation will add strength to the bank (Millar et al., 1993; Eaton, 2006; Braudrick et al., 2009; Tal and Paola, 2010) and hydraulic resistance causes more deposition of fines on the banks (Darby, 1999), so that the influence of the cohesive sediment on the banks can be important. These experimental results illustrate that bank strength by cohesive materials can be sufficient to sustain meander development even without the growth of vegetation as also observed on Mars (Howard, 2009).

5. Conclusions

A braided and a meandering gravel-bed river developed in our experimental flume study. For the first time, we conclusively linked the development of the different channel patterns to the formation of a cohesive floodplain and resulting bank stability. We conclude that the necessary conditions to form and sustain a meandering channel pattern are cohesive floodplain material and overbank flow in addition to a dynamic upstream perturbation. Results show that:

- Bank erosion rates decrease significantly for slightly cohesive floodplains, tested with systematic small-scale bank erosion rate tests.
- The braiding experiment is characterized by alternate bar formation in the initial straight channel, lateral channel migration and chute cutoff occurrence.
- Sustained lateral migration and cohesive floodplain formation results in a meandering river, without the occurrence of chute cutoffs. The cohesive floodplain stabilizes the banks, so that lateral bank migration and chute excavation decreases. Discharge variations are necessary to form a cohesive floodplain of overbank sedimentation on the higher outer banks and to fill potential chutes.
- The deposition of fines forms two styles of cohesive floodplains. First, a layer of cohesive material

on top of a non-cohesive bank in the outer bank, e.g. levees and crevasse splays. Second, lateral accretion of different grain-sizes in the inner bend.

• The experiments show that a meandering river can develop without having an initial cohesive bank. This suggests that the formation of a cohesive floodplain can result in the transition from a braided to a meandering river.

Acknowledgments

This project is supported by the Netherlands Organisation for Scientific Research (NWO) (grant ALW-Vidi-864·08·007 to MGK) and funding by ExxonMobil Upstream Research (grant EM01734 to MGK and George Postma). Comments on an earlier draft and discussion by Willem Toonen, Hans Middelkoop and Marcel van der Perk greatly helped to improve the paper. We acknowledge two anonymous reviewers for comments that significantly improved the manuscript, and editor Stuart Lane and associate editor Fiona Kirkby for their helpful guidance. We are grateful for technical support by H. Markies, M. van Maarseveen, T. van der Gon-Netscher, C. Roosendaal and H. van der Meer. The authors contributed in the following proportions to conception and design, data collection, analysis and conclusions, and manuscript preparation: WMvD (40, 45, 70, 85%), WIvdL (20, 45, 0, 0%) and MGK (40, 10, 30, 15%).

References

Ashmore, P. (1991). Morphology and bed load pulses in braided, gravel-bed streams. *Geografiska Annaler. Series A, Physical Geography*, 73(1):37–52.

Ashmore, P. E. (2001). Braiding phenomena: Statics and kinematics. In Mosley, P. M., editor, *Gravel Bed Rivers V*, pages 95–120. New Zealand Hydrological Society, Christchurch, New Zealand.

Asselman, N. E. M. (1999). Suspended sediment dynamics in a large drainage basin: the River Rhine. *Hydrological Processes*, 13(10):1437–1450, doi:10.1002/(SICI)1099-1085(199907)13:10<1437::AID-HYP821>3.0.CO;2-J.

Bertoldi, W., Zanoni, L., and Tubino, M. (2009). Planform dynamics of braided streams. *Earth Surface Processes and Landforms*, 34:547–557, doi:10.1002/esp.1755.

Braudrick, C. A., Dietrich, W. E., Leverich, G. T., and Sklar, L. S. (2009). Experimental evidence for the conditions necessary to sustain meandering in coarse bedded rivers. *Proceedings of the National Academy of Sciences of the United States of America*, 106(40):16936–16941, doi:10.1073/pnas.0909417106.

Brierley, G. J., Ferguson, R. J., and Woolfe, K. J. (1997). What is a fluvial levee? *Sedimentary Geology*, 114:1–9, doi:10.1016/S0037-0738(97)00114-0.

Bristow, C. S., Skelly, R. L., and Ethridge, F. G. (1999). Crevasse splay from the rapidly aggrading, sand-bed, braided Niobrara River, Nebraska: effect of base-level rise. *Sedimentology*, 46:1029–1047, doi:10.1046/j.1365-3091.1999.00263.x.

Camporeale, C., Perona, P., Porporato, A., and Ridolfi, L. (2005). On the long-term behavior of meandering rivers. *Water Resources Research*, 41:W12403, doi:10.1029/2005WR004109.

Carbonneau, P. E., Lane, S. N., and Bergeron, N. E. (2006). Feature based image processing methods applied to bathymetric measurements from airborne remote sensing in fluvial environments. *Earth Surface Processes and Landforms*, 31:1413–1423, doi:10.1002/esp.1341.

Cazanacli, D. A. and Smith, N. D. (1998). A study of morphology and texture of natural levees-Cumberland Marshes, Saskatchewan, Canada. *Geomorphology*, 25:43–55, doi:10.1016/S0169-555X(98)00032-4.

Coleman, J. M. (1969). Brahmaputra River: channel processes and sedimentation. *Sedimentary Geology*, 3:129–239, doi:10.1016/0037-0738(69)90010-4.

Constantine, J. A., McLean, S. R., and Dunne, T. (2010). A mechanism of chute cutoff along large meandering rivers with uniform floodplain topography. *Geological Society of America Bulletin*, 122:855–869, doi:10.1130/B26560.1.

Crosato, A. and Mosselman, E. (2009). Simple physics-based predictor for the number of river bars and the transition between meandering and braiding. *Water Resources Research*, 45:W03424, doi:10.1029/2008WR007242.

Darby, S. E. (1999). Effect of riparian vegetation on flow resistance and flood potential. *Journal of Hydraulic Engineering*, 125(5):443–454, doi:10.1061/(ASCE)0733-9429(1999)125:5(443).

Darby, S. E., Gessler, D., and Thorne, C. R. (2000). A computer program for stability analysis of steep, cohesive riverbanks. *Earth Surface Processes and Landforms*, 25:175–190, doi:10.1002/(SICI)1096-9837(200002)25:2<175::AID-ESP74>3.0.CO;2-K.

Darby, S. E., Rinaldi, M., and Dapporto, S. (2007). Coupled simulations of fluvial erosion and mass wasting for cohesive river banks. *Journal of Geophysical Research*, 112:F03022, doi:10.1029/2006JF000722.

Darby, S. E., Trieu, H. Q., Carling, P. A., Sarkkula, J., Koponen, J., Kummu, M., Conlan, I., and Leyland, J. (2010). A physically based model to predict hydraulic erosion of fine-grained riverbanks: The role of form roughness in limiting erosion. *Journal of Geophysical Research*, 115:F04003, doi:10.1029/2010JF001708.

Eaton, B. C. (2006). Bank stability analysis for regime model of vegetated gravel bed rivers. *Earth Surface Processes and Landforms*, 31:1438–1444, doi:10.1022/esp.1364.

Egozi, R. and Ashmore, P. (2009). Experimental analysis of braided channel pattern response to increased discharge. *Journal of Geophysical Research*, 114:F02012, doi:10.1029/2008JF001099.

Erkens, G., Hoffman, T., Gerlach, R., and Klosterman, J. (2011). Complex fluvial repsonse to Lateglacial and Holocene allogenic forcing in the Lower Rhine Valley (Germany). *Quaternary Science Reviews*, 30:611–627, doi:10.1016/j.quascirev.2010.11.019.

Ferguson, R. (1987). Hydraulic and sedimentary controls of channel pattern. In Richards, K., editor, *River channels: environment and process*, Institute British Geographers Special Publication 18, pages 129–158, Oxford, UK. Blackwell.

Ferguson, R. J. and Brierley, G. J. (1999). Levee morphology and sedimentology along the lower Tuross River, south-eastern Australia. *Sedimentology*, 46:627–648, doi:10.1046/j.1365-3091.1999.00235.x.

Friedkin, J. (1945). *A laboratory study of the meandering of alluvial rivers*. U.S. Army Corps of Engineers, U.S. Waterways Experiment Station, Vicksburg, Mississippi, USA.

Frings, R. M., Kleinhans, M. G., and Vollmer, S. (2008). Disciminating between pore-filling load and bed-structure load: a new porosity-based method, exemplified for the river Rhine. *Sedimentology*, 55:1571–1593, doi:10.1111/j.1365-3091.2008.00958.x.

Frings, R. M., Schüttrumpf, H., and Vollmer, S. (2011). Verification of porosity predictors for fluvial sand-gravel deposits. *Water Resources Research*, 47:W07525, doi:10.1029/2010WR009690.

Furbish, D. J. (1988). River-bend curvature and migration: How are they related? *Geology*, 16:752–755, doi:10.1130/0091-7613(1988)016.

Gibling, M. R. and Davies, N. S. (2012). Palaeozoic landscapes shaped by plant evolution. *Nature Geoscience*, 5:99–105, doi:10.1038/NGEO1376.

Gran, K. and Paola, C. (2001). Riparian vegetation controls on braided stream dynamics. *Water Resources Research*, 37(12):3275–3283, doi:10.1029/2000WR000203.

Hickin, E. J. and Nanson, G. C. (1984). Lateral migration rates of river bends. *Journal of Hydraulic Engineering*, 110(11):1557–1567, doi:10.1061/(ASCE)0733-9429(1984)110:11(1557).

Hooke, J. M. (2003). River meander behaviour and instability: a framework for analysis. *Transactions of the Institute of British Geographers*, 28:238–253, doi:10.1111/1475-5661.00089.

Howard, A. D. (2009). How to make a meandering river. *Proceedings of the National Academy of Sciences of the United States of America*, 106(41):17245–17246, doi:10.1073/pnas.0910005106.

Ikeda, S., Parker, G., and Sawai, K. (1981). Bend theory of river meanders. Part 1. Linear development. *Journal of Fluid Mechanics*, 112:363–377, doi:10.1017/S0022112081000451.

Jackson, R. G. (1976). Depositional model of point bars in the Lower Wabash River. *Journal of Sedimentary Petrology*, 46:579–594, doi:10.1306/212F6FF5-2B24-11D7-8648000102C1865D.

Kean, J. W. and Smith, J. D. (2006a). From drag in rivers due to small-scale natural topographic features: 1. regular sequences. *Journal of Geophysical Research*, 111:F04009, doi:10.1029/2006JF000467.

Kean, J. W. and Smith, J. D. (2006b). From drag in rivers due to small-scale natural topographic features: 2. irregular sequences. *Journal of Geophysical Research*, 111:F04010, doi:10.1029/2006JF000490.

Kleinhans, M. G. (2010). Sorting out river channel patterns. *Progress in Physical Geography*, 34:287–326, doi:10.1177/0309133310365300.

Kleinhans, M. G., Schuurman, F., Bakx, W., and Markies, H. (2009). Meandering channel dynamics in highly cohesive sediment on an intertidal mud flat in the Westerschelde estuary, the Netherlands. *Geomorphology*, 105:261–276, doi:10.1016/j.geomorph.2008.10.005.

Kleinhans, M. G. and Van den Berg, J. H. (2011). River channel and bar patterns explained and predicted by an empirical and physics-based method. *Earth Surface Processes and Landforms*, 36:721–738, doi:10.1002/esp.2090.

Kleinhans, M. G., van Dijk, W. M., van de Lageweg, W. I., Hoendervoogt, R., Markies, H., and Schuurman, F. (2010). From nature to lab: scaling self-formed meandering and braided rivers. In Dittrich, Koll, Aberle, and Geisenhainer, editors, *Riverflow 2010, volume 2*, pages 1001–1010. Bundesanstalt fÃijr Wasserbau.

Kleinhans, M. G. and Van Rijn, L. C. (2002). Stochastic prediction of sediment transport in sand-gravel bed rivers. *Journal of Hydraulic Engineering*, 128(4):412–425, doi:10.1061/(ASCE)0733-9429(2002)128:4(412).

Langendoen, E. J. and Simon, A. (2008). Modelling the Evolution of Incised Streams. II: Streambank Erosion. *Journal of Hydraulic Engineering*, 134:905–915, doi:10.1061/(ASCE)0733-9429(2008)134:7(905).

Lauer, J. W. and Parker, G. (2008). Net local removal of floodplain sediment by river meandering migration. *Geomorphology*, 96:123–149, doi:doi:10.1016/j.geomorph.2007.08.003.

Leopold, L. B. and Wolman, M. G. (1957). *River channel patterns: braided, meandering and straight*, volume 282-B. Geological Survey Professional Paper.

Lewin, J. (1978). Floodplain geomorphology. *Progress in Physical Geography*, 2:408–437, doi:10.1177/030913337800200302.

Lewis, G. W. and Lewin, J. (1983). *Modern and Ancient Fluvial Systems*, volume 6, chapter Alluvial cutoffs in Wales and the Borderlands, pages 145–154. International Association of Sedimentologists Special Publication.

Lick, W., Jin, L., and Gailani, J. (2004). Initiation of movement of quartz particles. *Journal of Hydraulic Engineering*, 130:755–761, doi:10.1061/(ASCE)0733-9429(2004)130:8(755).

Makaske, B. (2001). Anastomosing rivers: a review of their classification, origin and sedimentary products. *Earth-Science Reviews*, 53:149–196, doi:10.1016/S0012-8252(00)00038-6.

Matsubara, Y., Howard, A. D., Burr, D. M., Moore, J. M., and Williams, R. M. (2011). A long term meander evolution simulation: A model evaluation using the field data from Quinn River, Nevada. In *AGU Fall Meeting Abstracts*, page B684. Provided by the SAO/NASA Astrophysics Data System.

Micheli, E. R. and Larsen, E. W. (2011). River channel cutoff dynamics, Sacramento river, California, USA. *River Research and Applications*, 27:328–344, doi:10.1002/rra.1360.

Middelkoop, H. and Asselman, N. E. M. (1998). Spatial variability of floodplain sedimentation at the event scale in the Rhine-Meuse delta, the Netherlands. *Earth Surface Processes and Landforms*, 23(6):561–573, doi:10.1002/(SICI)1096-9837(199806)23:6<561::AID-ESP870>3.0.CO;2-5.

Millar, R. G. (2000). Influence of bank vegetation on alluvial channel patterns. *Water Resources Research*, 36(4):1109–1118, doi:10.1029/1999WR900346.

Millar, R. G., Quick, M. C., and ASCE, M. (1993). Effect of bank stability on geometry of gravel rivers. *Journal of Hydraulic Engineering*, 119(12):1343–1363, doi:10.1061/(ASCE)0733-9429(1993)119:12(1343)).

Nanson, G. C. (1980). Point bar and floodplain formation of the meandering Beatton River, northeastern British Colombia, Canada. *Sedimentology*, 27:3–29.

Nanson, G. C. and Croke, J. C. (1992). A genetic classification of floodplains. *Geomorphology*, 4(6):459–486, doi:10.1016/0169-555X(92)90039-Q.

O'Brien, P. E. and Wells, A. T. (1986). A small, alluvial crevasse splay. *Journal of Sedimentary Petrology*, 56(6):876–879, doi:10.1306/212F8A71-2B24-11D7-8648000102C1865D.

Parker, G. (1979). Hydraulic geometry of active gravel rivers. *Journal of the Hydraulic Division, American Society of Civil Engineers*, 105(9):1185–1201.

Parker, G., Shimizu, Y., Wilkerson, G. V., Eke, E. C., Abad, J. D., Lauer, J. W., Paola, C., Dietrich, W. E., and Voller, V. R. (2011). A new framework for modeling the migration of meandering rivers. *Earth Surface Processes and Landforms*, 36(1):70–86, doi:10.1002/esp.2113.

Parker, G., Wilcock, P. R., Paola, C., Dietrich, W. E., and Pitlick, J. (2007). Physical basis for quasi-universal relations describing bankfull hydraulic geometry of single-thread gravel bed rivers. *Journal of Geophysical Research*, 112:F04005, doi:10.1029/2006JF000549.

Peakall, J., Ashworth, P. J., and Best, J. L. (2007). Meander-bend evolution, alluvial architecture, and the role of cohesion in sinuous river channels: a flume study. *Journal of Sedimentary Research*, 77(3):1–16, doi:10.2110/jsr.2007.017.

Pérez-Arlucea, M. and Smith, N. D. (1999). Depositional patterns following the 1870s avulsion of the Saskatchewan River (Cumberland Marshes, Saskatchewan, Canada). *Journal of Sedimentary Research*, 69(1):62–73, doi:10.2110/jsr.69.62.

Reinfeld, I. and Nanson, G. C. (1993). Formation of braided river floodplains, Waimakariri River, New Zealand. *Sedimentology*, 40(6):1113–1127, doi:10.1111/j.1365-3091.1993.tb01382.x.

Rinaldi, M. and Darby, S. E. (2008). 9 Modelling river-bank-erosion processes and mass failure mechanisms: progress towards fully coupled simulations. In Habersack, H. and PiÃl'gay, H. and Rinaldi, M., editor, *Gravel-Bed River VI: From Process Understanding to River Restoration*, volume 11, pages 213–233. Elsevier.

Rouse, H. (1937). Nomogram for the settling velocity of spheres. In *Division of Geology and Geography, Exhibit D of the Report of the Commission on Sedimentation, 1936-1937*, pages 57–64, Washington DC. National Research Council.

Schumm, S. A. and Khan, H. R. (1972). Experimental study of channel patterns. *Geological Society of America Bulletin*, 83(6):1755–1770, doi:10.1130/0016-7606(1972)83[1755:ESOCP]2.0.CO;2.

Simon, A. and Collinson, A. J. C. (2002). Quantifying the mechanical and hydrologic effects of riparian vegetation on streambank stability. *Earth Surface Processes and Landforms*, 27(5):527–546, doi:10.1002/esp.325.

Simon, A., Curini, A., Darby, S. E., and Langendoen, E. J. (2000). Bank and near-bank processes in an incised channel. *Geomorphology*, 35:193–217, doi:10.1016/S0169-555X(00)00036-2.

Smith, C. E. (1998). Modeling high sinuosity meanders in a small flume. *Geomorphology*, 25:19–30, doi:10.1016/S0169-555X(98)00029-4.

Struiksma, N., Olesen, K. W., Flokstra, C., and De Vriend, H. J. (1985). Bed deformation in curved alluvial channels. *Journal of Hydraulic Research*, 23(1):57–79, doi:10.1080/00221688509499377.

Tal, M. and Paola, C. (2010). Effects of vegetation on channel morphodynamics: Results and insights from laboratory experiments. *Earth Surface Processes and Landforms*, 35(9):1014–1028, doi:10.1002/esp.1908.

Thorne, C. R. (1982). Processes and mechanisms of river bank erosion. In Hey, R. D., Bathurst, J. C., and Thorne, C. R., editors, *Gravel-bed Rivers*, pages 227–259. John Wiley & Sons: Chichester.

Toonen, W. H. J., Kleinhans, M. G., and Cohen, K. M. (2012). Sedimentary architecture of abandoned channel fills. *Earth Surface Processes and Landforms*, 37:459–472, doi:10.1002/esp.3189.

Törnqvist, T. E. and Bridge, J. S. (2002). Spatial variation of overbank aggradation rate and its influence on avulsion frequency. *Sedimentology*, 49(5):891–905, doi:10.1046/j.1365-3091.2002.00478.x.

Van de Lageweg, W. I., Van Dijk, W. M., Hoendervoogt, R., and G., K. M. (2010). Effects of riparian vegetation on experimental channel dynamics. In Dittrich, Koll, Aberle, and Geisenhainer, editors, *Riverflow 2010, volume 2*, pages 1331–1338. Bundesanstalt fÃijr Wasserbau.

Van de Lageweg, W. I., Van Dijk, W. M., and Kleinhans, M. G. (2013). Channel belt architecture formed by an experimental meandering river. *Sedimentology*, 60:840–859, doi:10.1111/j.1365-3091.2012.01365.x.

Van Dijk, W. M., Van de Lageweg, W. I., and G., K. M. (2012). Experimental meandering river with chute cutoffs. *Journal of Geophysical Research*, 117(F3):F03023, doi:10.1029/2011JF002314.

Vandenberghe, J. (2003). Climate forcing of fluvial system development: an evolution of ideas. *Quaternary Science Reviews*, 22(20):2053–2060, doi:10.1016/S0277-3791(03)00213-0.

Vollmer, S. and Kleinhans, M. G. (2007). Predicting incipient motion including the effect of turbulent pressure fluctuations in the bed. *Water Resources Research*, 43:W05410, doi:doi:10.1029/2006WR004919.

Walling, D. and He, Q. (1997). Investigating spatial patterns of overbank sedimentation on river floodplains. *Water, Air and Soil Pollution*, 99:9–20, doi:10.1023/A:1018303609232.

Wilcock, R. P. and Southard, J. B. (1988). Experimental study of incipient motion in mixed-size sediment. *Water Resources Research*, 24(7):1137–1151, doi:10.1029/WR024i007p01137.

Zanke, U. C. E. (2003). On the influence of turbulence on the initiation of sediment motion. *International Journal of Sediment Research*, 18(1):17–31.

Zinger, J. A., Rhoads, B. L., and Best, J. L. (2011). Extreme sediment pulses generated by bend cutoffs along a large meandering river. *Nature Geoscience*, 4:675 – 678, doi:10.1038/NGEO1260.

Zwolinski, Z. (1992). Sedimentology and gemorphology of overbank flows on meandering river floodplains. *Geomorphology*, 4(6):367–379, doi:10.1016/0169-555X(92)90032-J.